

Department of the Interior  
U.S. Geological Survey

LS-IAS-07  
Version 1.0

LANDSAT 1-5 MULTISPECTRAL  
SCANNER (MSS) IMAGE ASSESSMENT  
SYSTEM (IAS) RADIOMETRIC  
ALGORITHM DESCRIPTION DOCUMENT (ADD)

Version 1.0  
June 2012









# Executive Summary

This Algorithm Description Document ([ADD](#)) defines the algorithms the United States Geological Survey ([USGS](#)) Earth Resource Observation and Science ([EROS](#)) Center uses for the radiometric processing of Landsat Multispectral Scanner ([MSS](#)) imagery. The Image Assessment System ([IAS](#)), release R10.2, uses the radiometric processing algorithms to generate Landsat 1 to Landsat 5 MSS Radiometrically Corrected data products.

This document is consistent with all other relevant requirements and interface documents connected with these systems.



# Document History

<b>Document Number</b>	<b>Document Version</b>	<b>Publication Date</b>	<b>Change Number</b>	<b>Status/Issue</b>
LS-IAS-07	Version 1.0	June 2012	DCR 380	



# Contents

<b>Executive Summary</b>	<b>iii</b>
<b>Document History</b>	<b>v</b>
<b>Contents</b>	<b>vii</b>
<b>List of Tables</b>	<b>xi</b>
<b>List of Figures</b>	<b>xiii</b>
<b>1 Introduction</b>	<b>1</b>
1.1 Purpose . . . . .	1
<b>2 Overview and Background</b>	<b>3</b>
2.1 Mission Objective . . . . .	4
2.2 MSS Historical Perspective . . . . .	4
<b>3 Instrument Description</b>	<b>7</b>
3.1 Relative Spectral Responses . . . . .	9
3.2 Quantization and Compression . . . . .	11
<b>4 Radiometric Processing Algorithm Flows</b>	<b>15</b>
<b>5 Extract Calibration Wedge Values</b>	<b>17</b>
5.1 Introduction . . . . .	17
5.2 Background . . . . .	18
5.2.1 MSS-X . . . . .	19
5.2.2 MSS-X WBVT . . . . .	19
5.2.3 MSS-X GSFC . . . . .	19

5.2.4	MSS-P	20
5.2.5	MSS-A	21
5.3	Inputs	21
5.4	Outputs	21
5.5	Outputs to Report File and Database	21
5.6	Calibration Wedge Data Decompression	22
5.7	Calibration Wedge Data Extraction	23
5.7.1	MSS-X Calibration Wedge Data Extraction	23
5.7.2	MSS-A Calibration Wedge Data Extraction	27
<b>6</b>	<b>Gain and Offset Calculation Algorithm</b>	<b>29</b>
<b>7</b>	<b>Scan Line Artifact (SLA) Detection (LMASK Population)</b>	<b>31</b>
7.1	Introduction	31
7.1.1	Dropped Lines	31
7.1.2	Scan-Line Amplification	32
7.1.3	Severe Detector Striping	33
7.1.4	Sticky Bit	33
7.1.5	Other	35
7.2	Inputs	35
7.3	Outputs	36
7.4	Outputs to Report File and Database	36
7.5	Algorithm	36
7.6	Issues	42
<b>8</b>	<b>SLA Detection Algorithm Part2</b>	<b>43</b>
8.1	Introduction	43
8.2	Background	43
8.3	Methodology	43
8.4	Inputs	45
8.5	Outputs	45
8.6	Algorithm	45
<b>9</b>	<b>Saturation Point Detection (LMASK Population)</b>	<b>49</b>
9.1	Introduction	49
9.2	Background	49
9.3	Inputs	49
9.4	Outputs	50

9.5	Outputs to Report File and Database . . . . .	50
9.6	Algorithm . . . . .	50
<b>10</b>	<b>Conversion from Qcal to Radiance Space</b>	<b>53</b>
10.1	Introduction . . . . .	53
10.2	Background . . . . .	53
10.3	Inputs . . . . .	54
10.4	Outputs . . . . .	54
10.5	Algorithm . . . . .	54
<b>11</b>	<b>Histogram Analysis MSS-P, Landsat 2–3</b>	<b>55</b>
11.1	Introduction . . . . .	55
11.2	Background . . . . .	55
11.3	Inputs . . . . .	56
11.3.1	Input Parameters from CPF . . . . .	56
11.4	Outputs to Report File and Database . . . . .	56
11.5	Algorithm Description . . . . .	57
11.6	Issues . . . . .	57
<b>12</b>	<b>Histogram Analysis MSS-X Format</b>	<b>59</b>
12.1	Introduction . . . . .	59
12.2	Background . . . . .	59
12.3	Inputs . . . . .	61
12.3.1	Input Parameters from CPF . . . . .	61
12.4	Outputs . . . . .	62
12.5	Outputs to Report File and Database . . . . .	64
12.6	Algorithm Description . . . . .	65
12.6.1	Daytime Input (L0R) Image Data . . . . .	65
12.6.2	L0c / L1R Reflective Band Image Data . . . . .	65
12.6.3	Daytime L0c/L1R Image Data (all bands) . . . . .	66
<b>13</b>	<b>Cross Calibration to L5 MSS</b>	<b>69</b>
13.1	Introduction . . . . .	69
13.2	Background . . . . .	69
13.3	Inputs . . . . .	72
13.4	Parameters Obtained From the CPF . . . . .	73
13.5	Outputs . . . . .	73
13.6	Database . . . . .	73

13.7	Algorithm . . . . .	73
<b>14</b>	<b>Absolute Gain and Offset Adjustment</b>	<b>75</b>
14.1	Introduction . . . . .	75
14.2	Background . . . . .	75
14.3	Methodology . . . . .	76
14.4	Inputs . . . . .	78
14.5	Parameters Obtained From the CPF . . . . .	78
14.6	Outputs . . . . .	78
14.7	Algorithm . . . . .	79
<b>15</b>	<b>Cosmetic De-Stripping</b>	<b>81</b>
15.1	Introduction . . . . .	81
15.2	Background . . . . .	81
15.3	Input Parameters from CPF . . . . .	81
15.4	CPF Parameters . . . . .	82
15.5	Outputs . . . . .	82
15.6	Algorithm Description . . . . .	83
	<b>Appendices</b>	<b>85</b>
	<b>Acronyms</b>	<b>87</b>
	<b>References</b>	<b>89</b>

# List of Tables

2.1	MSS Spectral Bands and their Applications [8] . . . . .	3
3.1	Wavelength of Each MSS Band Designation . . . . .	9
3.2	MSS Modes by Band . . . . .	14
11.1	Lmin – Lmax table for MSS . . . . .	56



# List of Figures

3.1	Landsat MSS Sensor Diagram . . . . .	7
3.2	Landsat MSS Detector Orientation to Ground Track . . . . .	8
3.3	MSS Active Scan Pattern with Respect to Direction of Flight . . . . .	10
3.4	Landsat MSS Detector Calibration Shutter Wheel Diagram . . . . .	10
3.5	Landsat 1 MSS Relative Spectral Responses . . . . .	11
3.6	Landsat 2 MSS Relative Spectral Responses . . . . .	12
3.7	Landsat 3 MSS Relative Spectral Responses . . . . .	12
3.8	Landsat 4 MSS Relative Spectral Responses . . . . .	13
3.9	Landsat 5 MSS Relative Spectral Responses . . . . .	13
4.1	Nominal MSS-P Day and Night Process Flow . . . . .	15
4.2	Nominal MSS-X and MSS-A Process Flow (under construction) . . . . .	16
5.1	MSS Video and Wedge Level Timing Sequence . . . . .	17
5.2	A Calibration Gray Wedge Showing Six Word Locations . . . . .	18
5.3	Decompression Curve Examples for Landsat 1 . . . . .	22
5.4	Calibration Wedge Data Before and After Data Filtration . . . . .	26
7.1	Example of a Dropped Line with Ringing Effect . . . . .	32
7.2	Example of a Dropped Line with Ringing Effect . . . . .	32
7.3	Pixel Value Profile Graph . . . . .	33
7.4	Example of Severe Detector Striping . . . . .	34
7.5	Example of Vertically Taken Pixel Value Profile . . . . .	34
7.6	Example of the Decoding ‘Sticky Bit’ Issue . . . . .	35
7.7	Example of SLA Flagged with Two Adjacent Lines for Step 1 . . . . .	38
7.8	Example of Entire Dropped Scan (SLA of all six detectors) . . . . .	41
8.1	Sampling of a Flagged Line . . . . .	46

12.1	MSS Radiometric Processing Flow . . . . .	60
14.1	Mosaic Image of a TM Scene and Three Hyperion Scenes used in Cross Calibration . . . . .	77

# 1 Introduction

## 1.1 Purpose

This document describes the radiometric processing algorithms and data flows used in the Landsat 1–5 [MSS IAS](#) Level 1 Product Generation System (LPGS) 11.2. These algorithms are implemented as part of the IAS Level 1 (L1) processing, radiometric characterization, and radiometric calibration software components. These algorithms create accurate products, characterize the MSS radiometric performance (noise, dynamic range, anomalies, etc.), and derive improved estimates of absolute and relative radiometric calibration parameters. These algorithms produce outputs stored in the IAS database and are routinely trended as part of the radiometric performance monitoring. This document also presents background material describing the Landsat 1–5 MSS sensors and their radiometric calibration devices.



## 2 Overview and Background

The Landsat MSS is a multi-band remote sensing image receiver onboard Landsat 1–5. MSS sensor, the oldest operational multispectral digital sensor, allows scientists to look back at the Earth’s surface and climate ten years before the introduction of the Thematic Mapper (TM) instrument. The multi-band sensor acquired images of the Earth through red, green, and Near Infrared (R, G, NIR) filters almost continuously from July 1972 to January 1999. The specific band designations of R+G+NIR(High)+NIR(Low) changed between Landsat 1–3 and Landsat 4–5 with the addition of the TM.

The MSS data scene size for all satellites is 170 kilometers (km) north-south by 185 km east-west despite the lower orbits of Landsat 4–5 through an adjustment of swath extension and resolution for a broader field-of-view. The Instantaneous Field of View (IFOV) for all bands is 79 meter (m); the Earth’s surface is sampled every 57 m across track and every 79 m along track, yielding a 57 by 79 m pixel. Landsat 1–3 followed a polar orbit with an 18 day repeat cycle. Due to the lower orbits, Landsat 4–5 followed a polar orbit with a 16 day

Landsat 1,2, and 3 Spectral Bands	Landsat 4 and 5 Spectral Bands	Use
Band 4 Green	Band 1 Green	Emphasizes sediment-laden water and delineates areas of shallow water.
Band 5 Red	Band 2 Red	Emphasizes cultural features.
Band 6 Near IR	Band 3 Near IR	Emphasizes a vegetation boundary between land and water, and landforms.
Band 7 Near IR	Band 4 Near IR	Penetrates atmospheric haze best, emphasizes vegetation, the boundary between land and water, and landforms.

Table 2.1. MSS Spectral Bands and their Applications [8]

repeat cycle.

## 2.1 Mission Objective

The objective of the Landsat MSS mission is to provide global, seasonally re-freshed, medium-resolution (79 m MSS) imagery of Earth's land areas from a near-polar, sun-synchronous orbit. These data:

- Enable 18-day coverage for locations around the world (Landsat 1–3)
- Enable 16-day coverage for locations around the world (Landsat 4–5)
- Cross-calibrate to other Landsat imagers
- Are absolutely calibrated to invariant ground sites, providing a consistent scientific utility and environmental record

The Calibration Analysts use the IAS radiometric algorithms described in this document to ensure that the radiometric behavior of the MSS is sufficiently characterized to meet the mission objectives.

## 2.2 MSS Historical Perspective

The Landsat Project was built after the wide success of the Nimbus meteorological observation satellites. Starting with its first Launch on July 23, 1972 aboard Earth Resources Technology Satellite 1 (ERTS-1, later named Landsat 1), the MSS instrument has been crucial to the Landsat Project. Built by Hughes Aircraft Corporation, this scanning spectroradiometric sensor was the backbone of the first three Landsat satellites' data acquisition. It was not until Landsat 4–5 that the MSS became subsidiary to the more advantageous TM. The MSS sensor was also the first global monitoring system that used multiple band data in a digital format.

During its history, the MSS image format has undergone several changes. The first MSS data format was distributed on tape and organized in a Band Interleaved by Pixel Pair (BIP2) format. Eventually, Band Interleaved by Pixel (BIP), Band Interleaved by Line (BIL), and Band Sequential (BSQ) formats evolved. The earlier BIP and BIL formats were designed to accommodate the limited storage, disk access rates, and processing speeds of earlier media and computers. All current formats are BSQ.

Current “Level 0” formats used as input into IAS 10.5 and LPGS 11.5 (released in the summer 2011) fall into four types: MSS-X Goddard Space Flight Center ([GSFC](#)), MSS-X Wide-Band Video Tape ([WBVT](#)), Multispectral Scanner – Archive Format (MSS-A), and Multispectral Scanner – Processed Format (MSS-P). These format types are archived on a scene-by-scene basis, and the calibration data are available for viewing.

MSS-X GSFC, MSS-A, and MSS-P formats are radiometrically corrected for bias values and detector gains. For the MSS-X WBVT format, functionality is implemented in IAS and LPGS to simulate the radiometry of the other formats. The MSS-X WBVT format is unique among these formats because it retains the full calibration wedge from the raw data stream. The MSS-X GSFC and MSS-A have six calibration points sampled from the full wedge. The calibration wedge and its use in radiometric processing are described in Section 5.

MSS-A (where ‘A’ means “archive source”) data were produced from 1981 until the end of MSS acquisitions and included all MSS imagery from Landsat 4–5. Similar to the MSS-X format, these data have been radiometrically corrected for existing bias values and detector gains. These data have not been geometrically corrected; therefore, the scan lines and per-detector radiometry is preserved.

MSS-P (where ‘P’ stands for “processed source”) data are different from the MSS-A and MSS-X because both the radiometry and geometry were modified. These images were resampled to a map projection and the scan-line offsets Scan Line Offset ([SLO](#)) were adjusted. MSS-P data do not have the calibration correction values stored with the data and the detector geometry no longer exists.



### 3 Instrument Description

The MSS instrument was mounted to the bus of Landsat 1–5. The MSS instrument used an oscillating mirror that scanned for light reflection from Earth’s surface through a ground-pointing telescope (not shown).

Each oscillation cycle took 33 milliseconds and had an angular displacement of  $\pm 2.89^\circ$  from nadir to the satellite’s orbital track. The mirror covered an angle of  $11.56^\circ$  in a lateral scan Angular Field of View (AFOV). This encompassed a swath length of 185 km (115 miles) across the orbital track from an orbital altitude of 917 km (~ 570 miles). During a near-instantaneous forward movement of the satellite along its orbital flight path, the mirror would sweep

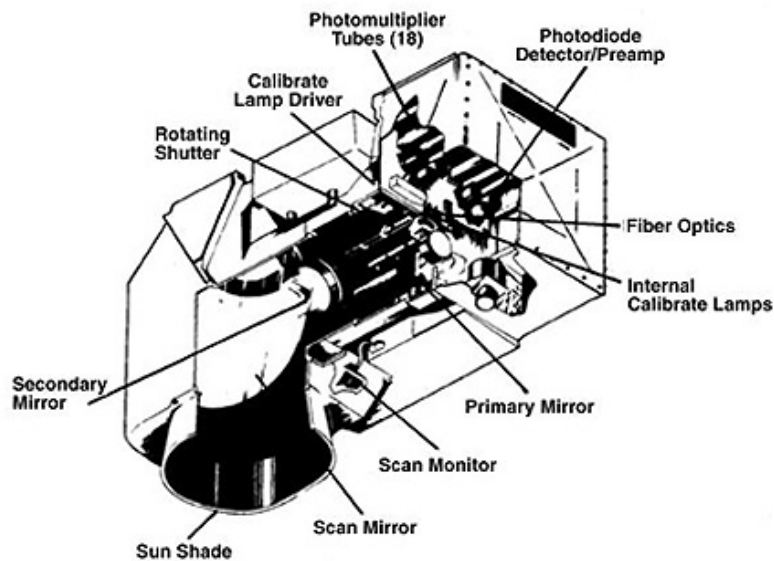


Figure 3.1. Landsat MSS Sensor Diagram

### MSS SCANNING ARRANGEMENT

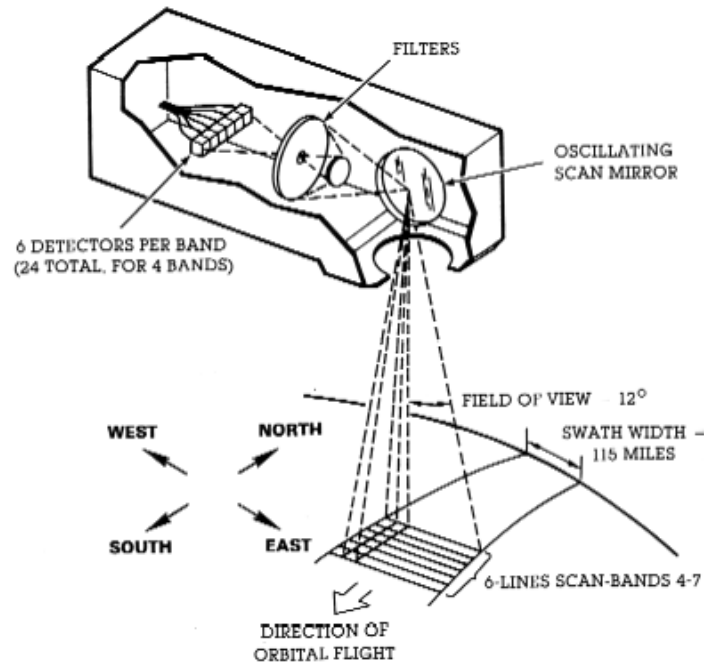


Figure 3.2. Landsat MSS Detector Orientation to Ground Track

laterally, covering a ground strip of  $\sim 474$  m (1554 ft) from one side of the track to the other. The mirror took about 16 milliseconds to complete each sweep. In the time it took to oscillate laterally, the spacecraft advanced 454 m relative to its ground track. In addition to this shifting by kinetic acquisition, through lateral oscillations of the AFOV, the Landsat satellites did not orbit in a perfect polar orbit. Landsat images are acquired at an orbital angle of  $99^\circ$  from the equator. This changes the orientation of the images' upper and lower margins a few degrees relative to perpendicular.

MSS collected four different filtered bandwidths of Earth-reflected solar radiance. These filtered bands were divided into green ( $0.6 - 0.7 \mu\text{m}$ ), red ( $0.5 - 0.6 \mu\text{m}$ ), NIR ( $0.7 - 0.8 \mu\text{m}$ ), and NIR ( $0.8 - 1.1 \mu\text{m}$ ) wavelengths.

The green, red, and first NIR bands used photomultiplier tubes as detectors; the second infrared sensor used silicon photodiodes. Each band filter consisted of six corresponding detectors that subdivided the across-track scan

Band designation in Landsat 1, 2, and 3	Band designation in Landsat 4 and 5	Spectral Range ( $\mu\text{m}$ )
4	1	0.5 – 0.6
5	2	0.6 – 0.7
6	3	0.7 – 0.8
7	4	0.8 – 1.1
8		10.4 – 12.5, Landsat 3 only <sup>a</sup>

<sup>a</sup>Considered the thermal band, deemed unsuccessful and not available.

Table 3.1. Wavelength of Each MSS Band Designation

into a parallel array. These detectors multiplied the signal before transmitting it back to Earth. Each detector had a ground width of approximately 79 m, and when added together, covered approximately 474 m (1555 ft) during each lateral scan. The satellites were designed to handle orbital speeds of approximately 26,611 km/h (16,525 mph), and the detectors collected image data at a rate of  $6.8 \times 10^{-6}$  m/s along the scan line. Light entered MSS through the optical lens of a ground pointing telescope as it reflected from the atmosphere and Earth's surface. The reflected light then passed through a train of mirrors and lenses where it divided and transported on fiber optics. The fiber optics conveyed the light to different filters where it separated into different spectral bands.

During the retrace swing of the sensor scan, the detector was exposed to a light source with a known radiometric output. The device consisted of a rotating disk that exposed a neutral density filter (prism), which projected light from calibrated tungsten lamp assemblies during each return oscillation. These steps calibrated all of the detectors between each scan swath to ensure consistent data. Photonic data was not collected during the retrace scan of the oscillating mirror because the ground width of the detector array was wide enough to overlap on the previous scan.

### 3.1 Relative Spectral Responses

Landsat 1–5 MSS instruments incorporated four spectral bands, as shown in Figure 3.5. These bands (1–4) were located on the primary focal plane and

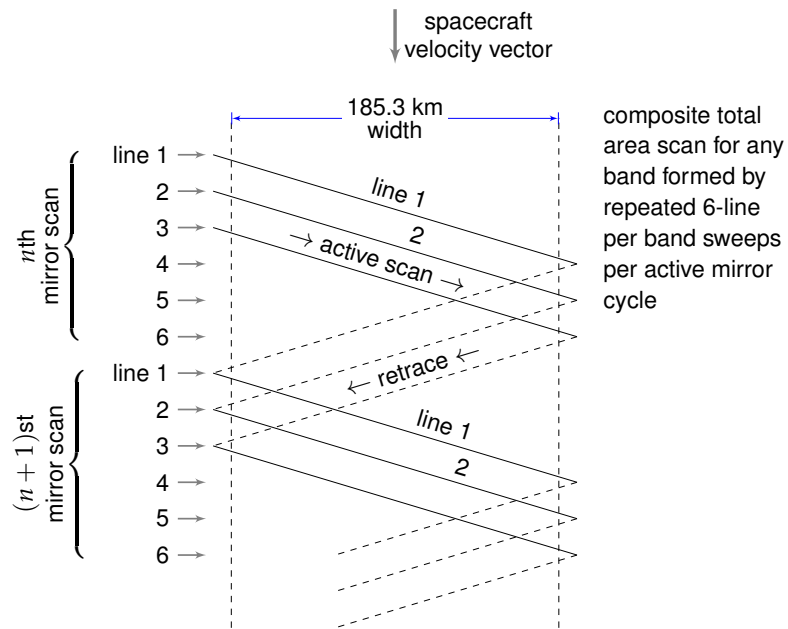


Figure 3.3. MSS Active Scan Pattern with Respect to Direction of Flight

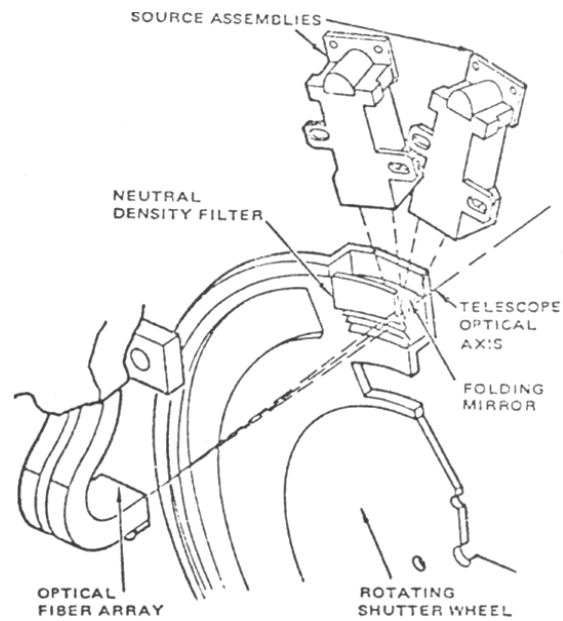


Figure 3.4. Landsat MSS Detector Calibration Shutter Wheel Diagram

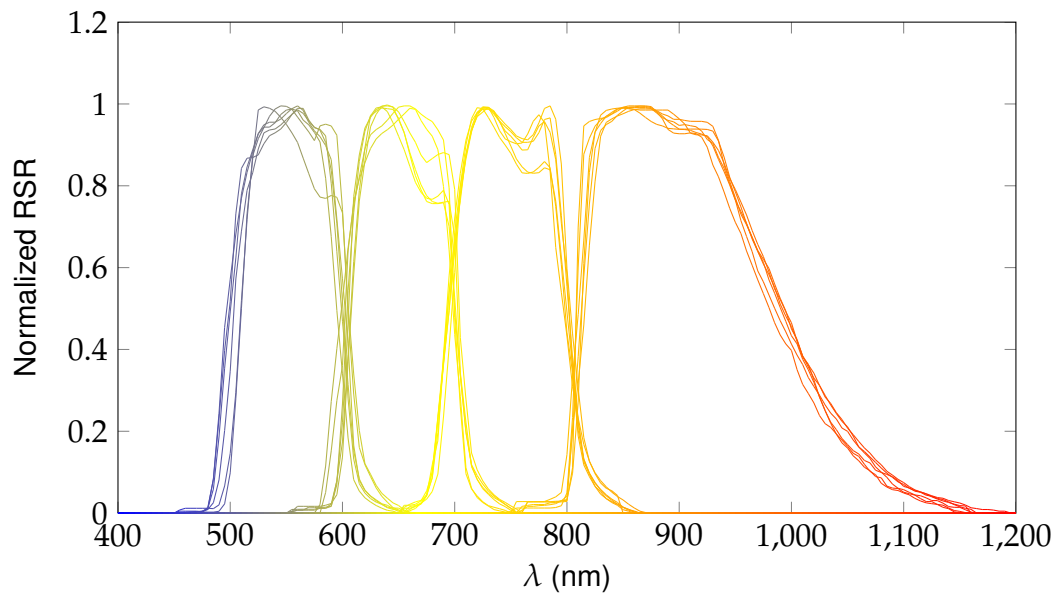


Figure 3.5. Landsat 1 MSS Relative Spectral Responses

covered the visible and NIR region. Differences exist between each band's six detectors, and the spectral overlap of each instrument.

### 3.2 Quantization and Compression

The video signal transfers to the analog-to-digital converter after quantization to 64 levels, either for direct (linear) encoding or through a signal compression amplifier prior to converting to digital form. The compression amplifier compresses the higher light levels and expands the lower light levels to nearly match the quantization noise to the photomultiplier detector noise. Photomultipliers have noise levels, which limit a system signal-to-noise performance at high light levels, but for low light levels, quantization noise becomes the limiting factor. Thus, the compression amplifier provides better signal-to-noise performance at low light levels.

The outputs of the 24 detectors are quantized into 64 levels, prior to transferring to the analog-to-digital converter for either direct (linear) encoding or through a signal compression amplifier prior to converting to digital form. These 64 quantum levels are evenly spaced across the entire 4-volt signal range. For

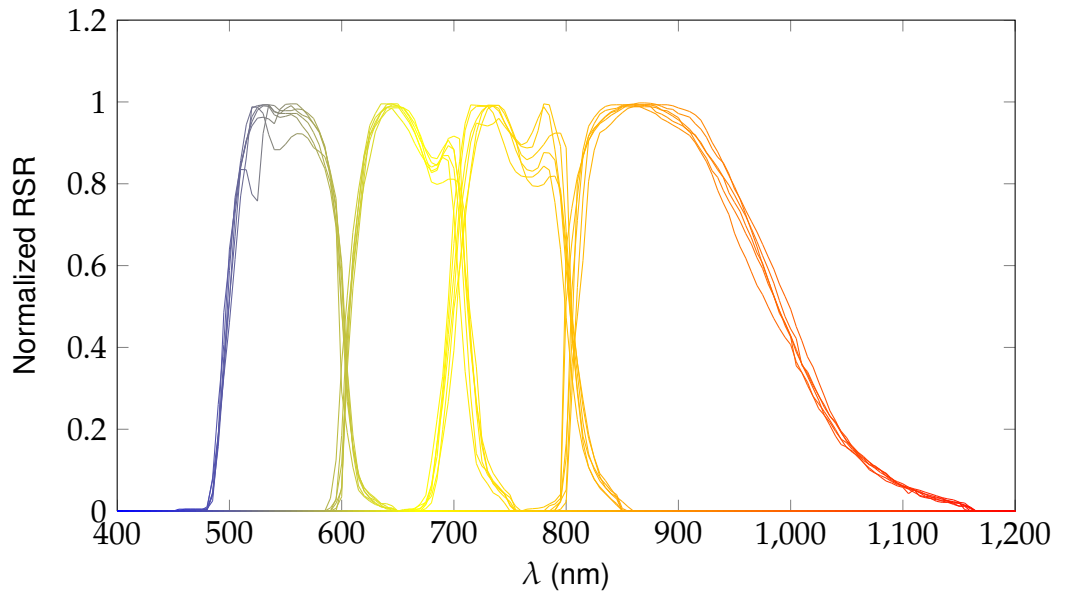


Figure 3.6. Landsat 2 MSS Relative Spectral Responses

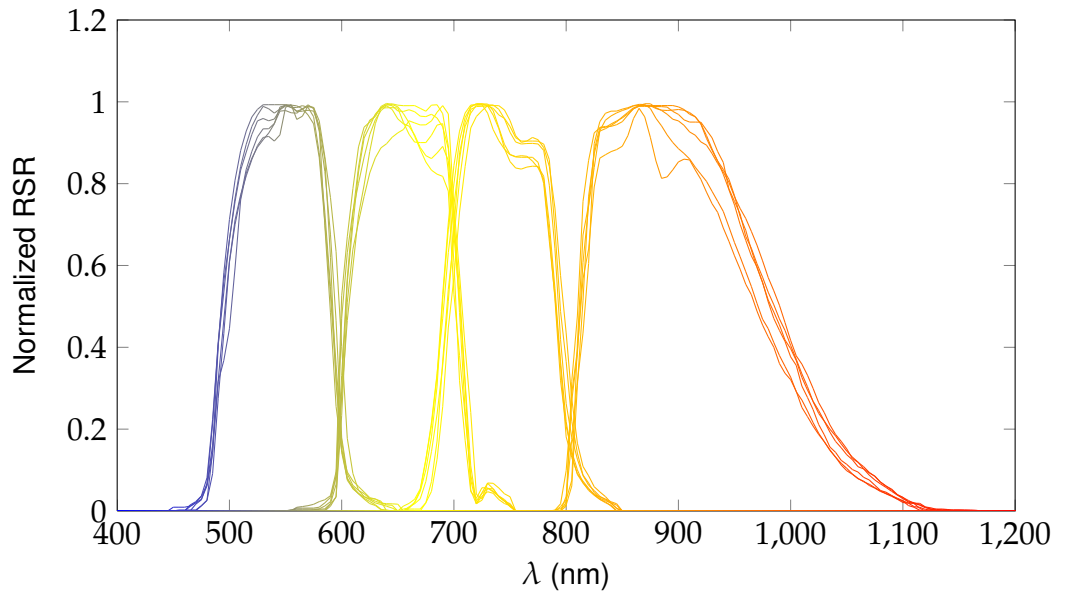


Figure 3.7. Landsat 3 MSS Relative Spectral Responses

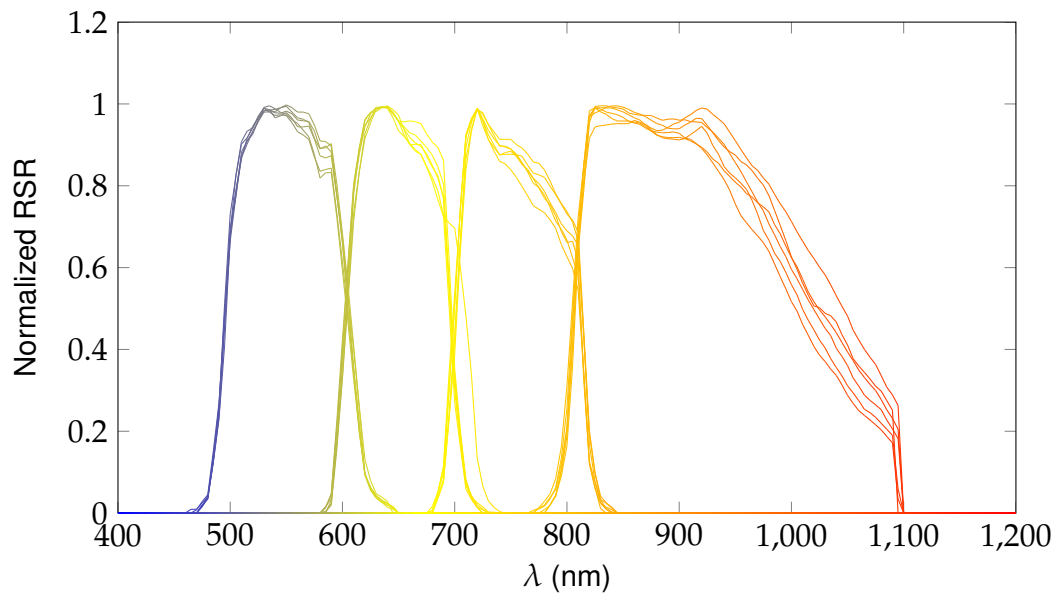


Figure 3.8. Landsat 4 MSS Relative Spectral Responses

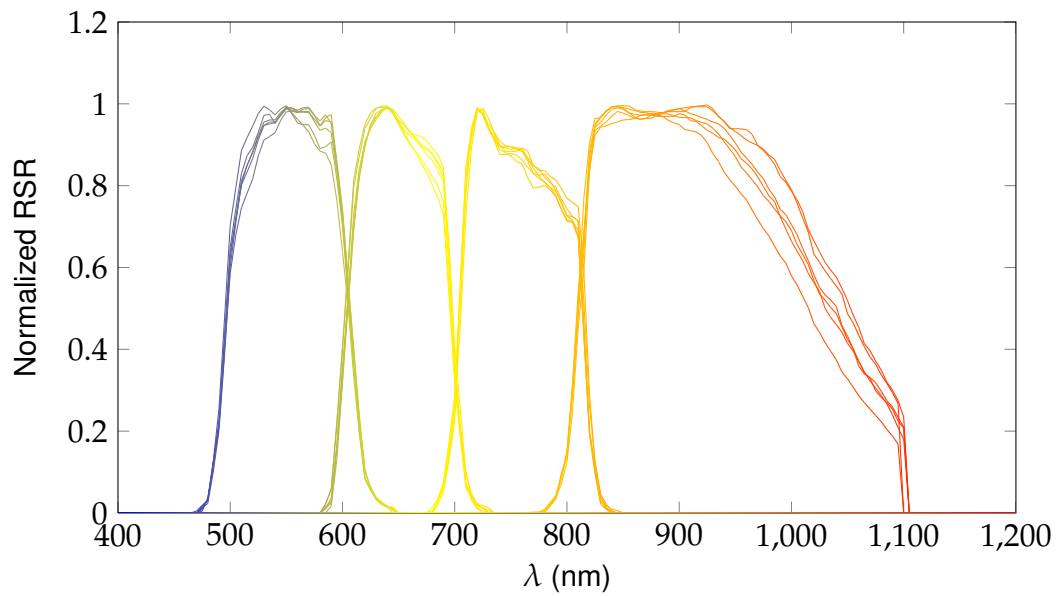


Figure 3.9. Landsat 5 MSS Relative Spectral Responses

Scanner Gain, Modes	Multiplexer Modes	
	Linear, Bands	Compression, Bands
High gain	1, 2	1, 2
Low gain	1, 2, 3, 4	1, 2, 3

Table 3.2. MSS Modes by Band

detectors 1 through 18 (comprising Bands 1, 2, and 3), this linear quantization scheme is not optimum because the noise in the signal diminishes as the square root of the signal. For example, a 4-volt signal contains twice as much rms noise as a 1-volt signal. For this reason, shaping the signal according to a square root law equalizes the noise throughout the range of the signal. After this process, a linear quantization matches the quantization errors precisely to the signal noise. The compression amplifier consists of four linear segments, which approximate the square root response curve.

Noise for the channels of Band 4 is established by the equivalent load resistor noise and is best matched by the direct (linear) quantization. For these six channels, the signal compression path is bypassed.

Gains in Bands 1-2 are commandable to the high gain mode, which provides an additional nominal gain increase of a factor of three. Table 3.2 shows the different available modes by band.

All four bands of the MSS-X WBVT format are 6-bit. Bands 4–6 are 7-bit and Band 7 is 6-bit for MSS-X GSFC. All needed file decompressions are no longer processed in MSS-X Archive Conversion System (MACS), and are performed in the IAS. Any files that need decompression are run through the decompression tables upon IAS input before any further processing occurs.

# 4 Radiometric Processing Algorithm Flows

Figure 4.1 displays the nominal MSS processing flow for radiometric correction of an MSS-P Level 0 scene. No scan line or detector radiometric calibration information is retained in the MSS-P data. The only radiometric information available is band histograms and statistics. Figure 4.2 displays the nominal MSS processing flow for radiometric correction of a Level 1 Radiometric (Corrected) (L1R) night scene.

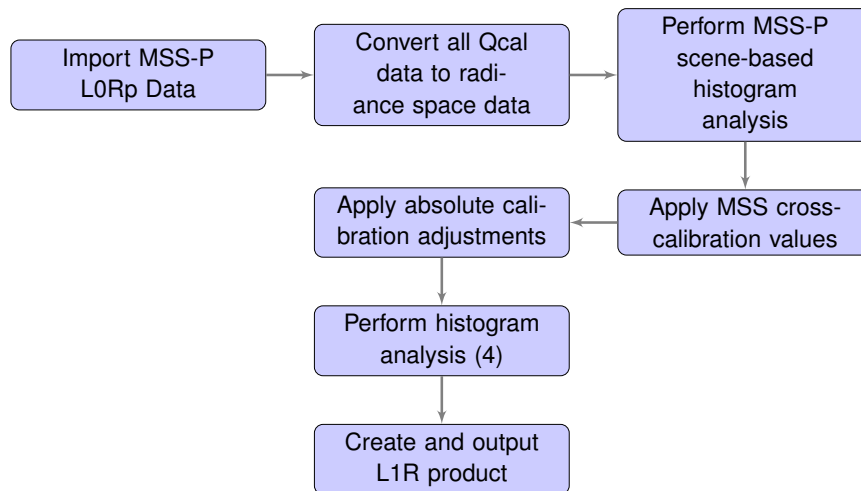


Figure 4.1. Nominal MSS-P Day and Night Process Flow

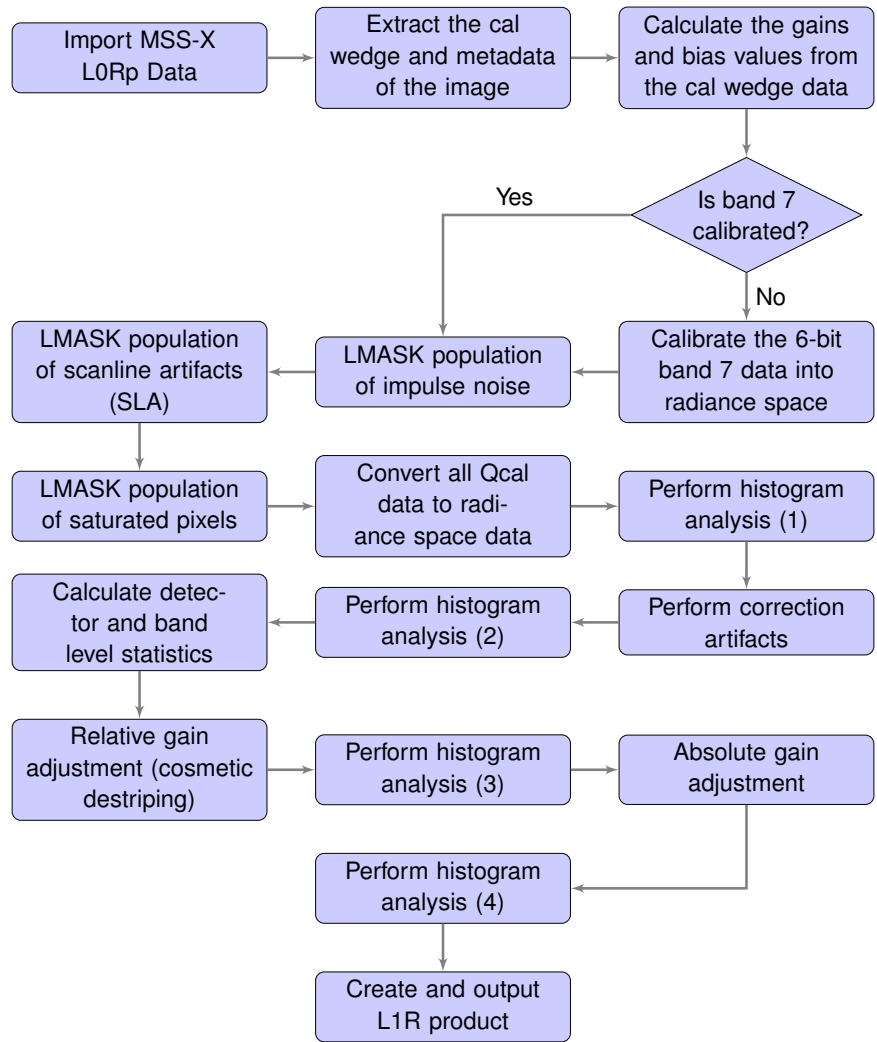


Figure 4.2. Nominal MSS-X and MSS-A Process Flow (under construction)

# 5 Extract Calibration Wedge Values

## 5.1 Introduction

All MSS systems performed a radiometric system stability analysis using an internal calibration lamp. One of two tungsten lamps, of known radiance, was used to calibrate the detectors during every other retrace swath (east to west). During this retrace scan, a shutter wheel blocked the Earth view from the optical fibers, and the calibration lamp was projected into the optical fibers through a variable neutral density filter on the shutter wheel.

This process produced a calibration wedge. In every alternate scan, the ground data processing system identified six locations in the calibration wedge, and the data from these locations were extracted (see Figure 5.2). In addition, a linear relationship between the input radiance ( $R_i$ ) and the output voltage ( $Q_i$ )

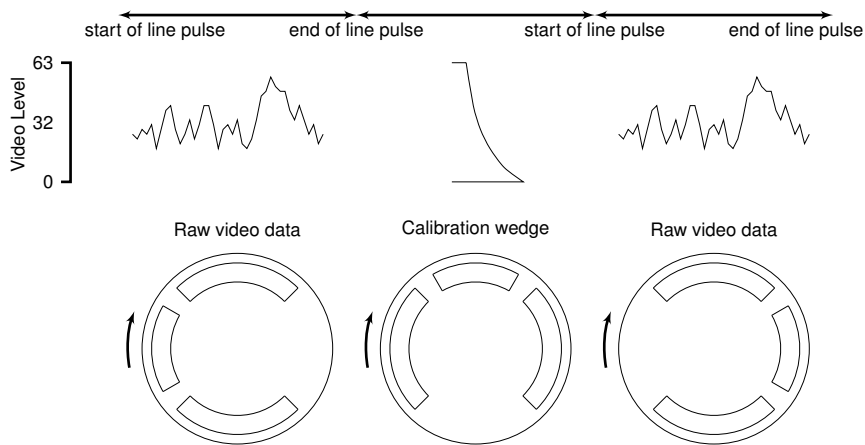


Figure 5.1. MSS Video and Wedge Level Timing Sequence

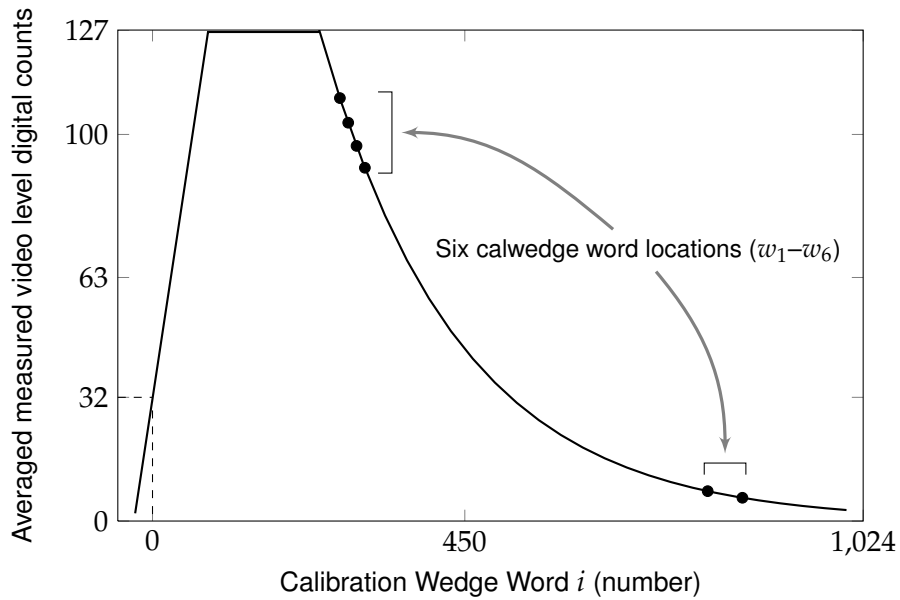


Figure 5.2. A Calibration Gray Wedge Showing Six Word Locations

existed. This relationship is given by the equation

$$Q_i = G_n R_i + O_n$$

where  $Q_i$  is the output voltage,  $R_i$  is the input radiance,  $G_n$  is the gain, and  $O_n$  is the offset.

To determine the corresponding data, detect the first value recorded on the rising edge greater than or equal to 32 Digital Number (DN), and record the values delayed by a specific number. The method of extracting internal calibration data for analysis depended on whether the full calibration wedge data, a sampled calibration wedge, or no usable calibration data were available.

## 5.2 Background

The full wedge is available for processing in the MSS-X WBVT data, while the six samples from the wedge are available for MSS-X GSFC and MSS-A data. Archived MSS data exists in four formats. The full wedges are categorized as MSS-X (WBVT and GSFC), MSS-P, and MSS-A. The calibration wedge data are quantized the same, either 6-bit or 7-bit, as the image data.

### **5.2.1 MSS-X**

The MSS-X data format includes all Landsat 1 data (collected from 1972 to 1976) and part of the Landsat 2-3 data (up to January 1979). These data are divided into an MSS-X GSFC format and a WBVT format. The primary difference between the two formats, excluding the sensor, was that Band 4 of the MSS-X GSFC format was not calibrated post launch, whereas the WBVT / MSS-X Band 4 data was calibrated post launch.

### **5.2.2 MSS-X WBVT**

MACS generated MSS-X WBVT data retains the full calibration wedge. The existence of the full calibration wedge for this format allows characterization of the calibration wedge and the historical calibration word (calibration word) extraction methods. Also, the existence of the full calibration wedge refined the calibration word extraction methods, and provided more accurate calculated gains and biases.

With IAS 10.5 and LPGS 11.5, the full calibration wedge is available for use in the MSS-X WBVT Level 0 format. The MSS-X GSFC 6 sample extraction process and radiometry is implemented in IAS 10.5 and LPGS 11.5 while further calibration wedge analysis is conducted.

### **5.2.3 MSS-X GSFC**

Bands 1–3 of the GSFC (or CCT-X) data had some radiometric processing / calibration performed, but Band 4 of the CCT-X data was never calibrated. Historically, six calibration words were read from the original calibration wedges before being discarded. For this reason, the only data available for the Band 4 calibration are the six historical calibration words.

MSS-X image data existed in a band sequential format with calibration data stored in a separate file, called the calibration data record. A single calibration data record contained calibration data associated with all four bands. Information was stored in the following format:

(Note: The location of a binary point is shown, where applicable.)

Field	Bytes	Format	Description
1	1 – 6	I	Band 4: 6 Calibration Wedge Samples
2	7 – 8	F	Band 4: Sun calibration Coefficient xxxx xxxx xxx.x xxxx
3	9 – 10	F	Band 4: Filtered Offset xxxx xxxx.xxxx xxxx
4	11 – 12	F	Band 4: Filtered Gain xxxx xxxx x.xxx xxxx
5	13 – 14	I	Band 4: Line Length Code
6	15 – 20	I	Band 5: 6 Calibration Wedge Samples
7	21 – 22	F	Band 5: Sun calibration Coefficient xxxx xxxx xxx.x xxxx
8	23 – 24	F	Band 5: Filtered Offset xxxx xxxx. xxxx xxxx
9	25 – 26	F	Band 5: Filtered Gain xxxx xxxx x.xxx xxxx
10	27 – 28	I	Band 5: Line Length Code
11	29 – 34	I	Band 6: 6 Calibration Wedge Samples
12	35 – 36	F	Band 6: Sun calibration Coefficient xxxx xxxx xxx.x xxxx
13	37 – 38	F	Band 6: Filtered Offset xxxx xxxx. xxxx xxxx
14	39 – 40	F	Band 6: Filtered Gain xxxx xxxx x.xxx xxxx
15	41 – 42	I	Band 6: Line Length Code
16	43 – 48	I	Band 7: 6 Calibration Wedge Samples
17	49 – 50	F	Band 7: Sun calibration Coefficient xxxx xxxx xxx.x xxxx
18	51 – 52	F	Band 7: Filtered Offset xxxx xxxx. xxxx xxxx
19	53 – 54	F	Band 7: Filtered Gain xxxx xxxx. xxxx xxxx
20	55 – 56	I	Band 7: Line Length Code

Note: Format type I represents integer values and format type F represents floating-point values.

## 5.2.4 MSS-P

From January 1979 through May 1981, the data Landsat 2–3 collected were archived in the MSS-P format. This format type was both radiometrically and geometrically corrected. Unfortunately, the method in which the MSS-P data was processed and archived left no calibration information to reference for further processing. The detector-specific information for each pixel and scan line was gone as well.

Note: A few MSS-A data scenes have been found during this time that can be used for analysis of MSS-P radiometry.

### 5.2.5 MSS-A

From June 1981 onward, all MSS data were archived in the MSS-A format, which included only radiometric corrections. All data from Landsat 4–5, including some data from Landsat 2–3, were archived in the MSS-A format. The MSS-A file structure consisted of the following files:

- Header
- Ancillary
- Annotation
- Trailer
- Image data (four bands of image data stored in band sequential format)

## 5.3 Inputs

- Decompression tables (CPF)
- $C'_i$  and  $D'_i$  tables (CPF)
- Maximum allowed calibration wedge line failure value D (work order)

## 5.4 Outputs

- Calculated gain and bias values from calibration wedge data
- Detector noise estimates

## 5.5 Outputs to Report File and Database

- Calibration wedge word values
- Average gain per detector
- Average bias per detector

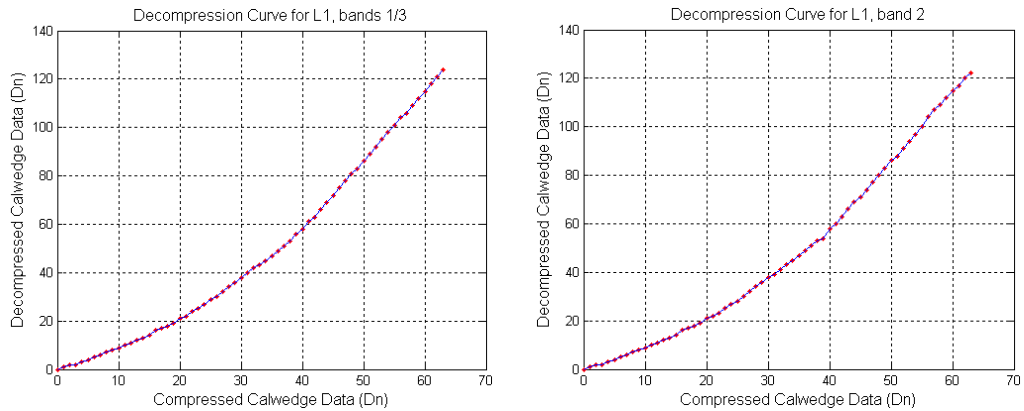


Figure 5.3. Decompression Curve Examples for Landsat 1

- Standard deviation of gains per detector
- Standard deviation of biases per detector
- Detector number of failed calibration wedge lines
- Total number of failed calibration wedge lines per band
- Total number of failed calibration wedge lines per detector

## 5.6 Calibration Wedge Data Decompression

Bands 1–3 were compressed before transmitting to the Ground Station, whereas Band 4 was transmitted linearly. Therefore, the calibration wedge data in Bands 1–3 must first be decompressed before further analysis. The decompression took place through the decompression tables found in the Calibration Parameter Files (CPFs) for Landsat 1–5.

Figure 5.3 illustrates an example of the decompression curves for Landsat 1. In this example, Bands 1–3 use the curve in the first plot while Band 2 uses the decompression curve in the second plot. Similar decompression curves exist for the rest of Landsat.

## 5.7 Calibration Wedge Data Extraction

### 5.7.1 MSS-X Calibration Wedge Data Extraction

MSS-X WBVT scenes all have the historically extracted calibration words and the full calibration wedge data available for image calibration. Due to the limitations of the historical calibration word extraction method, each WBVT image is backed out of its original calibration and then recalibrated using a new set of calibration words systematically extracted from the calibration wedge data. These new calibration words are calculated from a third-order curve that fit to the smoothed calibration wedge data and not the calibration wedge. The proper gain-state is established before the curve fits to the falling edge of the calibration wedge; therefore, the calibration words are extracted from the correct places along the curve. However, if good calibration words cannot be extracted from the calibration wedge, for any reason, then the image is flagged as a second-quality scene and a set of historical database averaged calibration word values are used to calibrate the scene.

MSS-X WBVT calibration performs the following steps:

1. The scene is input into IAS from MACS.
2. calibration words and calibration wedge data are extracted from a calibration file.
3. Image data are backed out of calibration using historical calibration words.
4. To open calibration wedge data and establish gain state, detect the duration of saturation before the falling edge of each wedge.
5. Determine the beginning pixel of the falling edge.
6. Run the low-pass filter on calibration wedge pixels to remove noise.
7. Fit a third-order curve to the falling edge of the calibration wedge.
8. Extract calibration words from proper places along the calibration curve (calibration curve).
9. Run statistical analysis on calibration wedge and new calibration words to determine their legitimacy.

10. If calibration words pass the legitimacy test, then use the calibration words to calibrate the image.
11. If calibration words fail the legitimacy test, then use the historical database average calibration word set to calibrate the image.

MSS-X GSFC data contain the calibration wedge data in a separate file. This file is called the Calibration Data Record (CDR), and the size of this record is  $56 \times 2340$  bytes. Every 56 bytes of this file contains 14 bytes of calibration data associated with each band (i.e., starting at Band 1 Detector 1, continuing to Band 2 Detector 1, Band 3 Detector 1, Band 4 Detector 1, Band 1 Detector 2, Band 2 Detector 2, etc.).

After the calibration wedge data have been extracted, numerous anomalies in the MSS-X data are observed. To adjust for these anomalies, a data filtering algorithm categorizes and directs the different issues to the appropriate correction algorithms. The following filtering conditions properly select valid data or reject invalid data from the CDR.

**Fifteen Bytes Block** Each CDR should contain  $56 \times 2340$  bytes. Within every 56 bytes is a representation of all four bands where 14 bytes correspond to each band. Out of these 14 bytes, the first 6 bytes correspond to the six calibration wedge words. The calibration wedge data corresponding to the six calibration wedge words are extracted by picking the first 6 bytes from the 14 bytes and storing this data for the particular band and detector. This process is repeated until all calibration wedge words are extracted and stored for all detectors over all four bands.

On occasion, 15 bytes of data can be observed instead of the normal 14 byte block. Normally, all data bytes in the CDR are appended one after the other making it difficult to locate the starting byte of the calibration wedge words. This can also create questions regarding the correct selection of the six calibration wedge words. A filter must be used to ensure the correct extraction of the six calibration wedge words from a 14 or 15 byte block. In this case, the decimal values eight and zero are historically stored as the sun calibration coefficients right after the six calibration wedge words. Instead of extracting the first 6 bytes as calibration wedge words, the sun calibration coefficients can be used as a reference to correctly identify the start of the six calibration wedge words. To correctly extract the six calibration wedge words from each band of each

CDR, two bytes are read at a time and checked for the 'eight and zero' consecutive bytes. Using this method ensures a correct extraction of the six calibration wedge words even if the 15 byte issue is encountered because the six bytes of data above these two bytes are read and stored as the valid calibration wedge words. This two byte reading process of the CDR continues until all data bytes are read and calibration wedge words stored for all detectors across all four bands.

**$w_i > w_{i+1}$**  Six calibration wedge words are selected from the trailing edge of the calibration gray wedge, where  $w_{i+1}$  should always be less than  $w_i$  and where  $i$  ranges from one to five. This implies that word-1 has the highest DN value, while word-6 has the lowest DN value. While extracting the calibration wedge words, some scans have calibration wedge words where  $w_i$  is less than  $w_{i+1}$ . This suggests an error in the data. Whenever a scan with this data anomaly is encountered, the entire scan is filtered out.

**$w_i = 0$**  Some scans have one of the calibration wedge words stored as zero. Whenever zero is encountered, all data from those six calibration wedge words are filtered out from further analysis.

**$w_i = 8$  and  $w_{i+1} = 0$**  Occasionally, data from six calibration wedge words contain consecutive words stored as eight and zero. This consecutive calibration gray wedge data are matched with sun calibration coefficients. Because this two-byte combination for the sun calibration coefficients is used as a reference to extract the calibration gray wedge data, the corrupted calibration wedge data with consecutive words creates confusion in selecting six calibration wedge values. Logic filters out the scan where two consecutive calibration wedge words are stored as eight and zero. In this special case, an assumption is made that there should be at least a 12-byte gap between two sun calibration coefficients. With each sun calibration coefficient, the number of data bytes read is counted before the next encounter of these two words (i.e., eight and zero). If the number of data bytes between the two sun calibration coefficients is less than 12, these words (eight and zero) are not the sun calibration coefficients but the corrupted calibration data stored in CDR. In this case, the usual process of picking the upper six bytes of data as calibration wedge words are not done, and the data byte reading and counting process continues until the next eight and zero consecutive values are read. This process continues unless the number of data bytes read between two consecu-

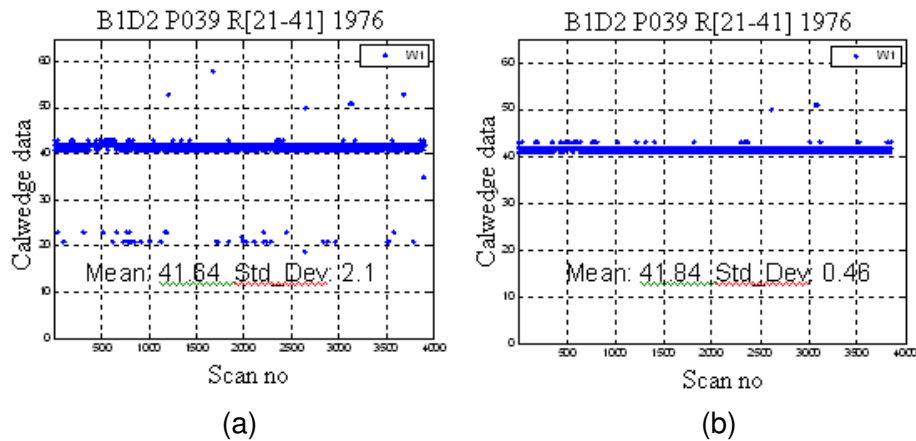


Figure 5.4. Calibration Wedge Data Before and After Data Filtration

tive sun calibration coefficients is at least twelve. Only the upper six bytes of data before approaching sun calibration coefficients are extracted and stored as calibration wedge words.

**Calibration Wedge Data Duplication Anomaly** Internal calibration data with six calibration wedge words are collected every two image scans. Every alternate scan of calibration wedge data is either filled with 63 DN, 21 DN, or with a duplicate value from the previous scan. Due to this anomaly, only the odd scans are selected to correctly pick the calibration wedge data values. Some consecutive scan lines of data sets do not maintain duplication. In these special cases, only the odd scan lines are used to pick the calibration wedge words and the even scans are disregarded.

Other anomalies may exist in the MSS-X data formats, which are yet to be recognized and studied; however the anomalies mentioned have been identified and categorized for correction. One unseen possibility of an uncategorized anomaly could be a very high value in the calibration wedge word in relation to its neighbor word (i.e., 5, 6, etc.). However, this issue could be identified after final filtration.

Figure 5.4 depicts the MSS-X calibration wedge data plot for Landsat 1 as a function of scan number over an interval before and after applying the data filtering algorithm. Figure 5.4(a) shows some data scattered around 20 to 25 DN and some data above 50 DN with the bulk of the data around 40 DN. Figure 5.4(b) shows that after applying the data filtering algorithm with the

filtering conditions explained before, most of the data above 50 DN and below 30 DN are filtered out.

## **5.7.2 MSS-A Calibration Wedge Data Extraction**

For the MSS-A data format, the internal calibration data are stored in the image file. The scans that do not contain calibration wedge data are filled with duplicate values from the previous scan. A few special cases occur during the calibration wedge data extraction and analysis where this occurrence is untrue. Six detectors are available for each band. Therefore, every six scan lines correspond to each of the six detectors. The calibration wedge words start at word-1 with the highest DN and proceed to word-6 with the lowest DN. The six words are contained in samples 3578 to 3583 in the image data. For each detector over a single scene, 400 (for 400 scan lines) calibration wedge data values exist for every six words with 200 unique values. Only one set of calibration wedge words is extracted for analysis, and the duplicate words are filtered out. The image data are stored in a decompressed format for the first three bands while the internal calibration data are stored in a compressed format.



# 6 Gain and Offset Calculation Algorithm

This set of algorithms calculates the initial gains and bias estimates through regression coefficients,  $C'_i$  and  $D'_i$ , for all bands and sensors. Excluding the flagged calibration wedge sets previously mentioned, these values calibrate Landsat 1 Band 7 GSFC format, and are used for trending between all bands and sensors in the MSS IAS. In the case of failed calibration wedge sets for the Landsat 1 Band 7 GSFC format, the interpolated values across the two nearest unflagged lines are used. To keep from interpolating across excessive calibration wedge failures, a predetermined value  $D$  establishes the number of lines that can fail before a scene fails. If a greater number of calibration wedge lines, value  $D$  fail, then abort the image with an error log. This value  $D$  is defined by the work order, and can be adjusted when needed.

```
if  $D < \sum$  flagged lines then
  Continue with processing.
else
  Drop the scene from processing.
end if
```

where, flagged line = 1 count.

Note: If the flagged calibration wedge line is located on the very top or bottom of the image, then use the value of the nearest good calibration wedge.

If scene processing continues, then

$$\hat{a} = \sum_i^6 C'_i V_i \quad b = \sum_i^6 D'_i V_i$$

where,  $\hat{a}$  is the smoothed bias value,  $b$  is the smoothed gain value,  $V_i$  are the calibration wedge values, and  $C_i$  and  $D_i$  are the regression coefficients from the prelaunch absolute radiometric calibration tables.

The second algorithm is a Kalman filter, which smooth the initial gains and biases of any detector noise.

Initial biases filter:

$$\hat{a}_s(1) = \hat{a}(1)$$

$$\hat{a}_s(n) = \hat{a}_s(n-1) + \begin{cases} \frac{1}{n} [\hat{a}(n) - \hat{a}_s(n-1)] & \text{for } 1 < n < N \\ \frac{1}{N} [\hat{a}(n) - \hat{a}_s(n-1)] & \text{for } n > N \end{cases}$$

Initial gains filter:

$$b_s(1) = b(1)$$

$$b_s(n) = b_s(n-1) + \begin{cases} \frac{1}{n} [b(n) - b_s(n-1)] & \text{for } 1 < n < N \\ \frac{1}{N} [b(n) - b_s(n-1)] & \text{for } n > N \end{cases}$$

where  $N$  is the length of the moving average filter window,  $n$  is the number of the calibration wedge values obtained from every other scan,  $\hat{a}$  are the initial bias values,  $b$  are the initial gain values,  $\hat{a}^s$  are the smoothed bias values, and  $b_s$  are the smoothed gain values.

# 7 Scan Line Artifact (SLA) Detection (LMASK Population)

## 7.1 Introduction

MSS imagery is stippled with system, sensor, and processing anomalies that appear in the scan data. If these artifacts appear within a single line and band, they can be associated with a particular detector, scan issue, or event. The process of finding these anomalies is called Scan Line Artifact (SLA) detection. SLAs are a group of pixels along a detector's acquisition swath / scan where the sensor's radiometric representation of its target is lost or amplified due to system errors. These artifacts are often caused by noise introduction from an outside source, an internal system error during data acquisition, data transfer interruptions, or data processing issues.

SLAs for MSS imagery often include, but are not confined to, the following items:

- Dropped lines
- Scan line amplification
- Severe detector striping ("Guitar String")
- Archive-tape reading issue ("Sticky Bit")
- Other (additional undefined artifacts in the data)

### 7.1.1 Dropped Lines

Dropped lines or partially dropped lines are created when a detector saturates during a scan swath, producing useless data. The line reads into the image as

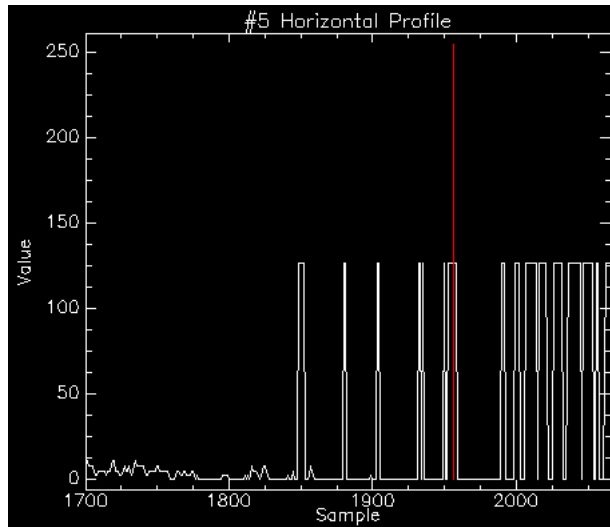


Figure 7.1. Example of a Dropped Line with Ringing Effect

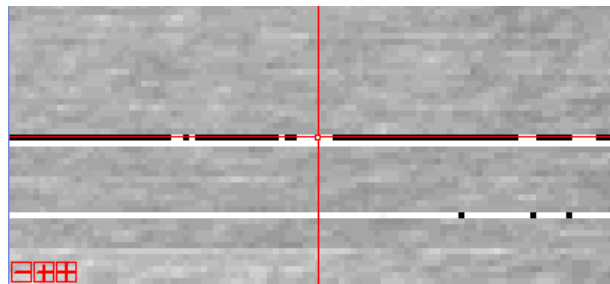


Figure 7.2. Example of a Dropped Line with Ringing Effect

either a saturated high or low string of pixels. These saturated lines can also bounce around between minimum (0) and maximum pixel values producing a ringing effect (127 for 7-bit MSS).

### 7.1.2 Scan-Line Amplification

Scan line amplification is an SLA where a detector's response is magnified along its scan. No determination has been made as to when this artifact occurs, but the anomaly causes the detector to jump to a higher response where the higher radiance values are truncated into high-end saturation.

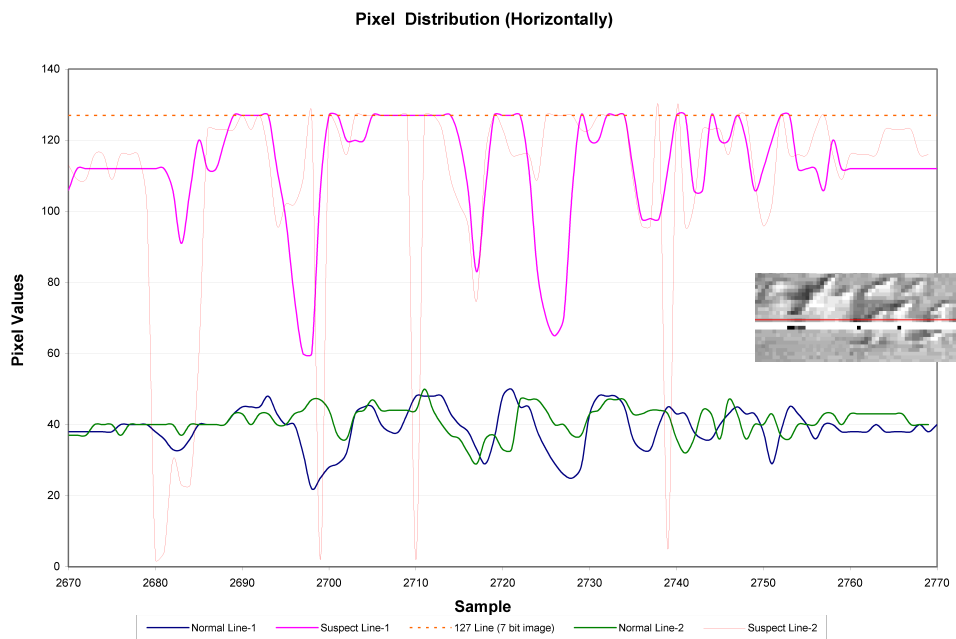


Figure 7.3. Pixel Value Profile Graph

Figure 7.3 displays a pixel value profile graph of two amplified lines matched against the adjacent ‘normal’ scan lines in the homogeneous region.

### 7.1.3 Severe Detector Striping

Severe detector striping is created when one of the detectors in a band acquires data samples at a higher or lower radiance than its adjacent detectors. These SLA(s) appear as an extreme difference of radiance values. Most of these lines are corrected during the relative gain correction phase of processing, but the LMASK SLA detection algorithm captures the extreme cases. The SLA only occurs in one detector (every sixth line).

### 7.1.4 Sticky Bit

It is believed that an archive-tape reading issue, dubbed ‘sticky-bit’, occurs when one of the bits “sticks” during the reading of archived files from high density tapes. This possible sticking bit causes a diagonal path of saturated pixels

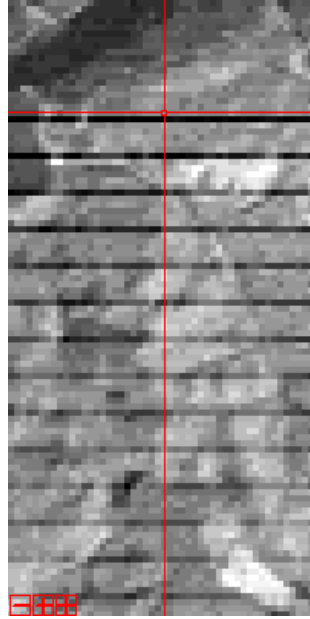


Figure 7.4. Example of Severe Detector Striping

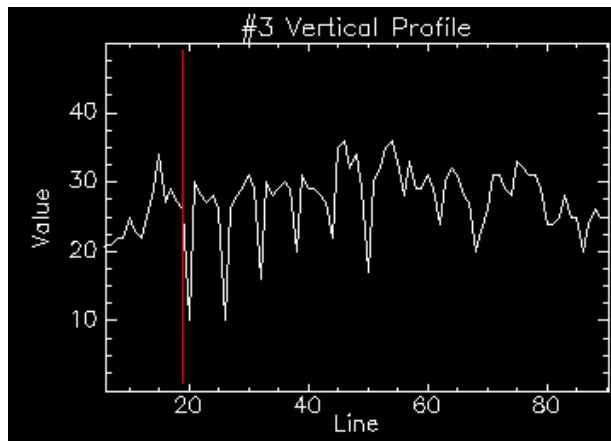


Figure 7.5. Example of Vertically Taken Pixel Value Profile

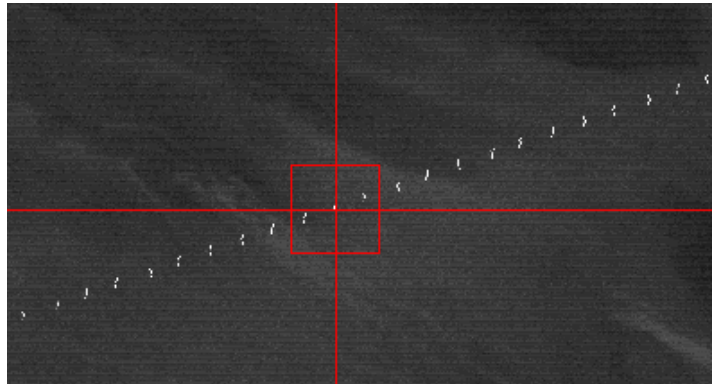


Figure 7.6. Example of the Decoding 'Sticky Bit' Issue

to form across the image, as illustrated in Figure 7.6. Effects of this particular anomaly are removed during the Saturation Detection stage of the LMASK processing.

### 7.1.5 Other

This is a placeholder for any additional SLA(s) that exist, but have not yet been identified.

The LMASK SLA detection keeps these artifacts from propagating into the scan line and histogram statistics.

## 7.2 Inputs

- Level 0 Reformatted Product (L0Rp) MSS-X Qcal data
- L0Rp MSS-A Qcal data
- Z – value (confidence interval) (work order(WO))
- $\sigma_T$  – threshold (WO)
- F band failure percentage value (WO)

## 7.3 Outputs

- SLA flagged line LMASK
- SLA processing report file

## 7.4 Outputs to Report File and Database

- Scene and band number of SLA(s)
- Line / detector number of SLA(s)
- Number of pixels (future release)
- SLA categorization type (future release)

## 7.5 Algorithm

When comparing the means between lines  $k$  and  $k + 1$ , the detection algorithm uses a Z-test at a selected confidence interval that the WO specifies. This computation checks for differences (termed “lag”) in the mean values from scan line to scan line. If the line is statistically different from its adjacent neighbor line using a preset confidence level, then that line is flagged as a possible problematic line. If the line fits within the confidence level of its neighbors, then it is tagged as unflagged ( $uf$ ).

1. The calculation in Equation 7.1 is the standard deviation of line  $L_k$  from its mean. This calculated line-specific standard deviation proves or disproves the null hypothesis in the Z-test of Equation 7.3.

In a detailed calculation of the Z-test, the standard deviation of each line is:

$$\sigma_k^2 = \frac{\sum_{i=1}^n (L_k(i) - \bar{L}_k)^2}{n_k - 1} \quad (7.1)$$

where  $\sigma_k^2$  is the standard deviation of line  $L_k$ ,  $n_k$  is the number of samples within line  $L_k$ ,  $i$  is the sample number,  $k$  is the line number,  $L$  is the sample line, and  $\bar{L}_k$  is the mean value of  $L_k$ .

2. Comparison of means and standard deviations between line  $L_k$  and its adjacent line  $L_{k+1}$  using the Z-test at a selected confidence interval (Z-value from WO).

$$\begin{aligned} H_0 : \overline{L}_k &= \overline{L}_{k+1}(uf + f) \\ H_1 : \overline{L}_k &\neq \overline{L}_{k+1}(f) \end{aligned} \quad (7.2)$$

where  $H_0$  is the Null hypothesis (observed truth),  $H_1$  is the alternate hypothesis (suggestive truth),  $k$  is the line number,  $\overline{L}_k$  is the mean value of the sample line  $L_k$ ,  $\overline{L}_{k+1}$  is the mean value of the adjacent sample line  $L_{k+1}$ ,  $uf$  is unflagged, and  $f$  is flagged.

To complete the Z-test, substitute the mean and standard deviation values calculated above into Equation 7.3.

$$|\overline{L}_{k+1} - \overline{L}_k| \geq Z \sqrt{\frac{\sigma_k^2}{n_k}} \quad (7.3)$$

If the condition shown in Equation 7.3 is satisfied, then the null hypothesis is rejected in favor of the alternate hypothesis. This demonstrates that the two lines are dissimilar. Therefore, both lines are flagged until further analysis determines whether they are SLA(s).

In order to reach a particular confidence interval, the Z-values should be less than or equal to the chosen Z-value defined in the WO. When the means of adjacent lines are within the confidence interval, they are assumed to be non-problematic and are not flagged. However, if the means of adjacent lines are not within the confidence interval, then it is flagged and marked as an SLA along with the two adjacent lines. Figure 7.7 illustrates flagging an SLA and the two adjacent lines.

3. After the lines have been flagged, a determination must be performed on whether the flagged lines are SLA(s). This step generates the values used to find the expected lag (difference) values across each line. The expected lags are compared with the actual lags, or differences, across the flagged rows to distinguish which lines are SLA(s) and which lines are good scans.

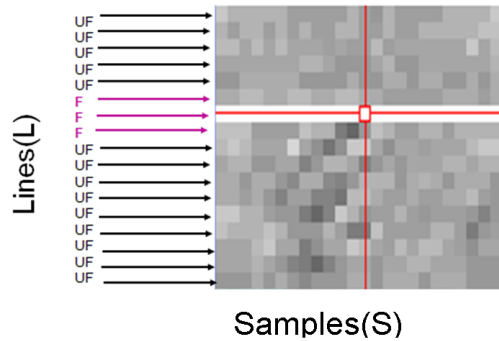


Figure 7.7. Example of SLA Flagged with Two Adjacent Lines for Step 1

Calculate the sum of lag for the flagged lines and unflagged lines (excluding background fill and/or non-image data, such as time stamps, etc.).

$$\text{Lag}_k = \sum_{i=1}^{\text{total samples}} |L_k(i+1) - L_k(i)| \quad (7.4)$$

where  $k$  is the line number,  $i$  is the sample number,  $L$  is the sample line,  $\text{Lag}_f$  is a subset of  $\text{Lag}_k$  which are flagged,  $\text{Lag}_{uf}$  is a subset of  $\text{Lag}_k$  which are unflagged, and total samples is the number of pixel samples for each individual detector scan.

```

if line number  $k$  is flagged then
   $\text{Lag}_k = \text{Lag}_k^f$ 
else
   $\text{Lag}_k = \text{Lag}_k^{uf}$ 
end if

```

The separation of  $f$  and  $uf$  shows that the unflagged lines,  $k$ , are used to find the expected values of the flagged lines,  $k$ , in Equation 7.4.

4. Special case: If the sum of lag values is zero for any flagged or unflagged lines, then designate the value as SLA(s).

```

if  $\text{Lag}_k^f$  or  $\text{Lag}_k^{uf} = 0$  then
   $L_k = \text{SLA}$ 
end if

```

5. The standard deviation of the scenes lag ( $\sigma'$ ) is calculated from the lags summation of the unflagged lines in Equation 7.5. This  $\sigma'$  is multiplied by 3 to establish the threshold of  $\pm 3\sigma'$ .

$$\sigma = \sqrt{\frac{\sum_{k=1}^{\text{number of unflagged}} (\text{Lag}^{uf} - \overline{\text{Lag}^{uf}})^2}{\text{number of unflagged} - 1}} \quad (7.5)$$

where  $k$  is the line number,  $\text{Lag}^{uf}$  are the lags of the unflagged lines,  $\overline{\text{Lag}^{uf}}$  is the average lag of the unflagged lines,  $\sigma'$  is the standard deviation of lag between the observed lines, and number of unflagged is the number of unflagged scan lines after step 4.

6. Because of their close relationship with relative gain differences, small SLA(s) must be dealt with in a cautious manner. If the scene's  $\sigma'$  value is smaller than the preset  $\sigma_T$ , then the value is set equal to  $\sigma_T$ . This action sets a minimal threshold to refrain from falsely flagging lines in homogeneous scenes where the  $\sigma'$  value is too small to distinguish between relative gain differences.

Checked:

**if**  $\sigma' < \sigma_T$  **then**  
     Set  $\sigma' = \sigma_T$ .  
**end if**

7. Find the nearest unflagged lines (a and b) adjacent to each flagged line. If the lag cannot be found from the above or below unflagged lines (in the case of a top-of-scene or bottom-of-scene flagged line), then the nearest unflagged lag ( $\text{Lag}_{ak}^{uf}$  or  $\text{Lag}_{bk}^{uf}$ ) is used exclusively. This step is needed in order to calculate an expected value for a flagged line using the average value of lines a and b.

Calculation of the nearest unflagged lines for every flagged line:

$$\text{Lag}_{ak}^{uf} = \text{Nearest } \text{Lag}^{uf} \text{ below } \text{Lag}_k^f$$

$$\text{Lag}_{bk}^{uf} = \text{Nearest } \text{Lag}^{uf} \text{ above } \text{Lag}_k^f$$

where  $k$  is the line number,  $\text{Lag}_{ak}^{uf}$  is the nearest first unflagged scan line above the flagged SLA(s), and  $\text{Lag}_{bk}^{uf}$  is the nearest first unflagged scan line below the flagged SLA(s).

8. The lag of the unflagged lines creates a trending line of the scene's variability for the  $3\sigma'$  threshold to follow. This action ensures that the SLA detection algorithm does not truncate high-end or low-end features, such as clouds or water bodies.

Calculate the expected value of lag (see Equation 7.6) for every flagged line from the nearest unflagged line above and nearest unflagged line below. The exception is if there is no unflagged line above (such as for the top line or when there are no unflagged lines above), then use the nearest unflagged line below exclusively. Similarly, if there is no unflagged line below, then use the unflagged line above exclusively.

Note: Extensive work with variograms has determined that the nearest unflagged line is the best method to identify lag between lines. Therefore, a limit of distance has not been placed between unflagged lines a and b. Weighting factors have also been disregarded because of the increasing confidence level needed to deal with the increasing distances between unflagged lines.

$$\text{Lag}_e^f = \frac{1}{2} \left( \text{Lag}_{ak}^{uf} + \text{Lag}_{bk}^{uf} \right) \quad (7.6)$$

where  $\text{Lag}_e^f$  is the expected sum of lag from the nearest unflagged line means,  $\text{Lag}_{ak}^{uf}$  is the nearest first unflagged scan line above the flagged SLA(s), and  $\text{Lag}_{bk}^{uf}$  is the nearest first unflagged scan line below the flagged SLA(s).

Figure 7.8 displays an example of an entire dropped scan (SLA of all detectors).

9. The SLA threshold sorts the falsely flagged lines from the SLA(s) through the use of the  $3\sigma'$  threshold. If the sum of lag for the flagged lines  $\text{Lag}_k^f$  is greater or less than  $\text{Lag}_e^f \pm 3\sigma'$ , then the scan line is marked as an SLA; otherwise, the scan line is a normal line.

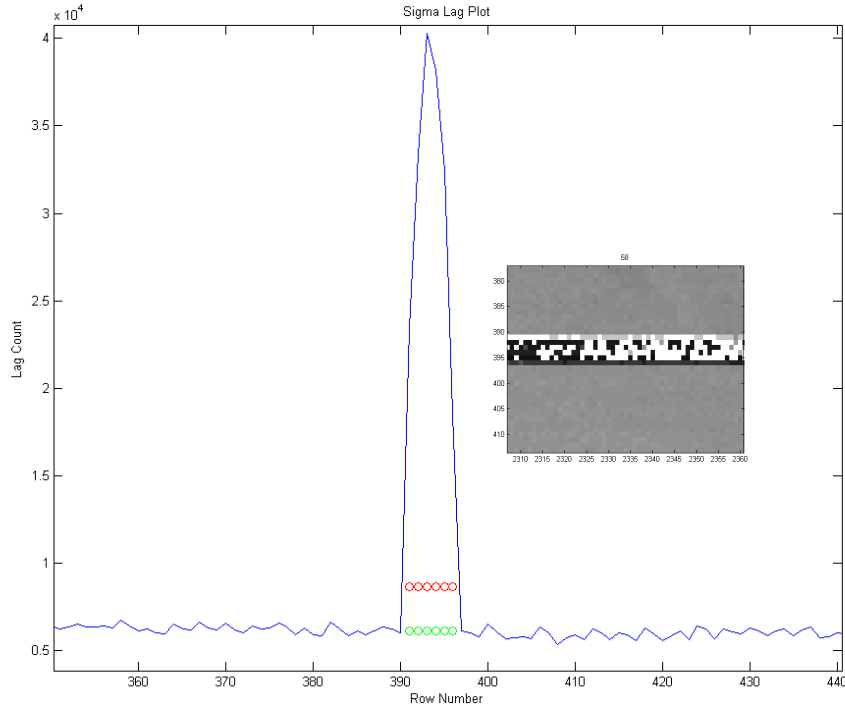


Figure 7.8. Example of Entire Dropped Scan (SLA of all six detectors)

If the condition is true:

$$\text{Lag}_k^f > \text{Lag}_e^f + 3\sigma' \quad (\text{Line is an SLA})$$

$$\text{Lag}_k^f < \text{Lag}_e^f - 3\sigma' \quad (\text{Line is an SLA})$$

$$\text{Lag}_e^f - 3\sigma' \leq \text{Lag}_k^f \leq \text{Lag}_e^f \quad (\text{Line is normal})$$

10. The final check for each scene band is a percentage failure assessment. If the SLA(s) of a band equals a larger percentage of the scene's scans than what the WO allows on a preset Failure ( $F$ ) percentage value, the image band is abandoned from the processing queue with an error report. From this point, the next image in the queue begins processing. If the SLA detection algorithms run and the number of SLA(s) within the image is less than the maximum allowable SLA threshold percentage, then the

scene is sent through to the next processing step.

$$F' = \frac{\# \text{SLA(s)}}{\text{total scans}}$$

**if  $F' \leq F$  then**

Continue with processing.

**else if  $F' > F$  then**

Remove scene from queue.

**end if**

where  $F'$  is the percentage of SLA(s) within a band, #SLA(s) is the number of SLA(s) found within the band, and total scans is the total number of scan lines in the band.

## 7.6 Issues

Problems arise within special cases where the logic is reversed or the SLA(s) run into boundary conditions and edge effects. If there are more SLA(s) than good lines, a greater possibility exists of missing problematic scan lines. Also, edge effects can occur when the top or bottom scan lines are SLA(s). In this situation, no upper or lower adjacent unflagged lines are available to confirm that the scan line in question is an SLA. At least one top or bottom adjacent line to use as an unexpected line value. When there are several flagged lines in a row, starting at the top or bottom of the scene, then the lag value for the nearest unflagged line (above or below) is used as the expected lag for these scans. Although this method is far from perfect, it supplies a general value within  $3\sigma'$  of the nearest unflagged lag to test the flagged lines. This means that the probability of capturing an SLA on first or last scan is reduced.

# 8 SLA Detection Algorithm Part2

## 8.1 Introduction

This is an extension to the [SLA](#) detection algorithm discussed in Section 7. When all of the problematic scans have been identified (flagged), a secondary statistical analysis of each line is made to distinguish the good pixels from the bad pixels. This action allows the LMASK to cover only the problematic areas of each flagged line, and uses any good data in these lines in the scene's statistics.

## 8.2 Background

In the case of many MSS SLAs, the artifact does not run the entire length of the scan. By flagging the entire line when an SLA is detected, the legitimate data are kept from the histogram and scene statistics analysis along with the problematic data. To keep the legitimate data in the scene analysis, the data must first be separated from the SLA data. Characterization of the flagged line pixels is made through a statistical analysis of comparing the pixels of the nearest adjacent non-problematic scan lines.

## 8.3 Methodology

To separate the scans containing SLA(s) from the rest of the scans, the previous algorithm identifies the problematic scan's statistical difference from neighboring (non-problematic) scans. This algorithm uses a similar statistical characterization method, but focuses on each pixel instead of the scan line as a whole. The following calculations run on any scans that the previous SLA detection algorithm flagged:

1. For every flagged scan line that the SLA detection algorithm finds, pixel-by-pixel comparisons are made against the mean ( $M$ ) and standard deviation ( $\sigma$ ) of the closest upper two and lower two 'non-flagged' pixels. The threshold is set by WO value  $N$  multiplied by  $\sigma$ . If the flagged line pixel value is greater than the maximum threshold ( $N\sigma_{\max}$ ) or less than the minimum threshold ( $N\sigma_{\min}$ ) from the calculated mean ( $M$ ) of the four neighboring pixel values, then it is marked as an SLA pixel.
2. If the pixel value falls within the threshold ( $N\sigma_{\min} < \text{Pixel Value} < N\sigma_{\max}$ ) set around  $M$ , then the pixel is considered good.

Special conditions include having too many flagged lines in a row, the flagged line not having two unflagged lines above, the flagged line not having two unflagged lines below, and/or falsely marking pixel(s) due to dramatic changes in the scene's relief. In order to deal with these special conditions, the following steps are implemented:

1. In the condition of too many flagged lines in a row, the system ignores the characterization of these flagged lines. These multiple flagged lines are left 'as is' and kept out of any additional statistical calculations. The WO determines the number of allowed flagged lines in a row ( $\#Flagged_{\max}$ ).
2. In the boundary condition where the flagged line is at the top of the image or in the case where it does not have any (or enough) unflagged lines above, the four nearest unflagged lines below are used for calculating the mean ( $M$ ) and standard deviation ( $\sigma$ ). This method is used as long as the number of flagged lines in a row condition is met.
3. In the boundary condition where the flagged line is at the bottom of the image or in the case where it does not have any (or enough) unflagged lines below, the four nearest unflagged lines above are used for calculating the mean ( $M$ ) and standard deviation ( $\sigma$ ). This method is used as long as the number of flagged lines in a row condition is met.
4. Some situations occur where flagged line pixels are falsely marked as problematic due to dramatic changes in the scene's relief. These falsely marked pixels are usually under ten pixels in length. To account for these falsely marked pixels, a minimum pixel run of  $P_{\min}$ , must exist. This action also performs a general cleanup of scattered problem pixel groups that are too small in size and number to affect the final scene statistics. If the

run of pixels is fewer than this, then the pixels are marked as ‘good pixels’ and used in the calculations of scene and detector statistics.

5. If there is a ‘good pixel’ run between two problematic pixel runs that are both larger than  $P_{\min}$ , and if that run is smaller than  $G_{\max}$ , then the gap is filled in as problematic pixels. The radiometry of these pixels cannot be trusted, and should not be allowed into the final scene statistics.

## 8.4 Inputs

- LORp MSS-X Qcal data
- LORp MSS-A Qcal data
- N – Standard deviation multiplier (WO)
- #Flaggedmax – Number of allowed flagged lines in a row (WO)
- $P_{\min}$  – Minimum bad pixel run (WO)
- $G_{\max}$  – Maximum pixel run between bad pixel runs  $> P_{\min}$  (WO)

## 8.5 Outputs

- Localized SLA flagged line LMASK
- Localized SLA processing report file
- Number of removed pixels

## 8.6 Algorithm

This algorithm is a simple scan through each flagged line that characterizes good acquired pixels from problematic pixels.

To find the mean ( $M$ ) and standard deviation ( $\sigma$ ) from neighboring unflagged line pixels (UF#) (see Figure 8.1 for details):

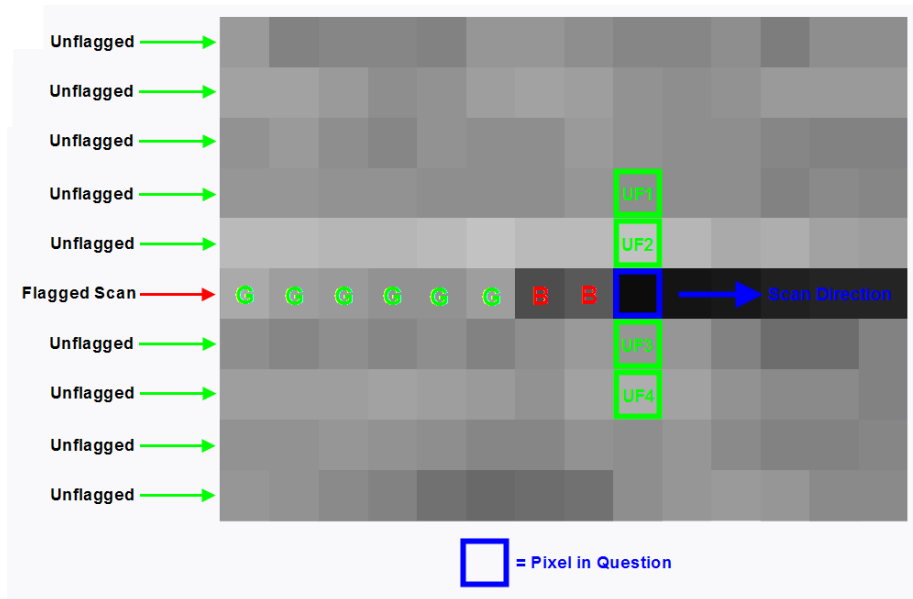


Figure 8.1. Sampling of a Flagged Line

$$M = \frac{UF1 + UF2 + UF3 + UF4}{n}$$

$$\sigma = \frac{\sum_{i=1}^n (UF\# - M)^2}{n - 1}$$

Where  $M$  is the mean,  $\sigma$  is the standard deviation,  $UF\#$  is a pixel from the neighboring unflagged line ( $UF1 \rightarrow UF4$ ), and  $n$  is the number of neighboring pixel samples ( $n = 4$ ).

In the normal case, unflagged neighboring pixel  $UF1$  is the second pixel directly above the flagged pixel in question, and unflagged neighboring pixel  $UF2$  is the pixel directly above the flagged pixel in question. This is similar for the two unflagged pixels directly below the pixel in question  $UF3$  (directly below) and  $UF4$  (second pixel below). See Figure 8.1 for details.

Figure 8.1 displays a sampling of a flagged line where each pixel is tested against its neighboring unflagged pixels. Passing the statistical tests marks the pixel in question as 'good' (G), and failing marks the pixel as 'bad' (B).

However, in the boundary condition where the flagged line is at the top of the image or in the case where the flagged lines do not have any (or enough)

unflagged lines above, the four nearest unflagged lines below are used for calculating the mean ( $M$ ) and standard deviation ( $\sigma$ ). In the boundary condition where the flagged line is at the bottom of the image or in the case where the flagged line does not have any (or enough) unflagged lines below, the four nearest unflagged lines above are used for calculating the mean ( $M$ ) and standard deviation ( $\sigma$ ). These methods are used as long as the number of flagged lines in a row condition are met.

The following lists the statistical conditions that the flagged pixels are checked against:

```

if number of flagged lines in a row > #Flaggedmax then
  Ignore
end if
if Pixel >  $M + \sigma N$  then
  Pixel = 'Bad pixel'
end if
if Pixel <  $M - \sigma N$  then
  Pixel = 'Bad pixel'
end if
if  $M + \sigma N > \text{Pixel} > M - \sigma N$  then
  Pixel = 'Good pixel'
end if
if Sum of consistent 'Bad pixels' <  $P_{\min}$  then
  'Bad Pixel' run = 'Good pixels'
end if
if Sum of consistent 'Good pixels' between 'Bad pixel' runs <  $G_{\max}$  then
  'Good pixel' run = 'Bad pixels'
end if

```



# 9 Saturation Point Detection (LMASK Population)

## 9.1 Introduction

This algorithm searches the MSS bands of each Landsat satellite for saturated data pixels. If the saturated pixels are not kept from the histogram analysis stages of processing, then the scene, band, and detector statistics would be thrown off. The algorithm searches for saturated pixels in the image and flags their location, which calculates the quality of the image.

## 9.2 Background

The MSS sensor bands had a functional dynamic range for top of atmosphere Top of Atmosphere (TOA) radiance collection. This radiance was captured by a series of detectors that gave a voltage response which was converted to a DN in accordance to that Band's dynamic range. In an attempt to reduce quantization, the dynamic range of each sensor was set for optimization of land feature collection. This optimization caused truncation of the high reflectance features such as clouds and white desert sands into the maximum DN. Because of its increased uncertainty due to this truncation, the max DN value (64 for 6-bit and 255 for 7-bit) cannot be trusted as a valid radiance-to-pixel representation. These pixels are then located and withheld from the histogram analysis to refrain from weighting the scene's statistical radiometric values.

## 9.3 Inputs

- MSS image matrix

## 9.4 Outputs

- Low saturated pixel LMASK
- High saturated pixel LMASK

## 9.5 Outputs to Report File and Database

- Number of low saturated pixels per detector scan
- Number of high saturated pixels per detector scan
- Number of low saturated pixels per band
- Number of high saturated pixels per band
- Average number of low saturated pixels per band
- Average number of high saturated pixels per band
- Average number of low saturated pixels per detector
- Average number of high saturated pixels per detector
- Standard deviation of low saturated pixels per band
- Standard deviation of high saturated pixels per band
- Standard deviation of low saturated pixels per detector
- Standard deviation of high saturated pixels per detector

## 9.6 Algorithm

1. For MSS-X and MSS-A images: Load the image data into a matrix and set the high-end and low-end saturation levels for the search. Depending on the data type, different amounts of blank space are left out. When the range of these blank spaces is predetermined, the tool gives a value of negative one to the pixels in this range. The pixels are given a value of

negative one because it is outside the 0 to 127 permitted values for the image data.

This action ensures that the saturated pixel locations found are not included in the blank spaces.

For MSS-P images: The blank spaces are not easily predicted. Therefore, there is no way to reduce the flagged pixels to within non-blank space range.

2. Search the image for 0 and 127 values. When a zero pixel value is found, the pixel's location is placed in a matrix for the low saturated pixels. When a 127 pixel value is found, the pixel's location is placed in a matrix for high saturated pixels.



# 10 Conversion from Qcal to Radiance Space

## 10.1 Introduction

This step converts the existing Qcal space MSS archive data (except for any Landsat 1 Band 7 data that have been calibrated in Section 1) into a non-quantized radiance space. This step allows the data to be closer to a true DN space and permits an unbiased sampling of existing detector values needed for the following algorithms of this document.

## 10.2 Background

All archived MSS data have been radiometrically processed. Relative gain adjustments have been calculated into all MSS formats prior to archiving, along with additional radiometric processing. The quantized, calibrated digital numbers, Qcal, represent these values. The digital numbers can be converted to spectral radiance or TOA radiance using known information. By converting the Qcal values to spectral radiance, a better representation of true spectral nature is obtained. This representation gives a better idea of what the satellite detectors originally acquisitioned.

All archived MSS-P imagery are L1R (Qcal radiance) products, and each of their four bands of Landsat 2–3 MSS-P imagery are archived in 7-bit format. This imagery format lost the detector-specific nature after being geometrically processed. This loss is due to a grid resampling of the pixels where the original radiance values have been replaced by interpolated values.

### 10.3 Inputs

- MSS archived Qcal space data
- Original QCAL  $L_{MIN\lambda} - L_{MAX\lambda}$  dynamic range values

### 10.4 Outputs

- Converted MSS radiance space data (floating-point)

### 10.5 Algorithm

This equation calculates the MSS archived Qcal data into radiance space.

$$L_{\lambda} = \frac{L_{MAX\lambda} - L_{MIN\lambda}}{QCALMAX} \times QCAL + L_{MIN\lambda}$$

Where  $L_{MIN\lambda}$  is the spectral radiance at  $QCAL = 0$ , and  $L_{MAX\lambda}$  is the spectral radiance at  $QCAL = QCALMAX = 127$  (for 7-bit data).

# 11 Histogram Analysis MSS-P, Landsat 2–3

## 11.1 Introduction

This algorithm extracts the relevant first- and second-order detector statistics from MSS-P image data. It is assumed that the MSS-P data have been converted from Qcal space into Spectral Radiance ( $\text{W}/\text{m}^2 \cdot \text{sr} \cdot \mu\text{m}$ ) prior to performing the statistical calculations. These statistics can be used to determine the following:

- MSS-P band dynamic range utilization
- Validation that historical Lmin, Lmax values are appropriate

## 11.2 Background

This algorithm provides a limited level of functionality as compared to the Enhanced Thematic Mapper Plus ([ETM+](#)) and TM IAS implementations. The fundamental driver for the simplification is that MSS-P data no longer have detector unique characteristics, but instead have the detector data mixed via resampling. Thus, all statistical metrics are based on band level data. A further simplification is that this algorithm is intended to only run at one point in the Radiometric Processing Subsystem ([RPS](#)) process flow after the image data have been converted to spectral radiance, and before rescaling the data to pseudo Landsat 5 MSS product space. Due to lack of detector level information, relative gain calculations are also ignored.

Processing Dates	Band 4		Band 5		Band 6		Band 7	
	Lmin	Lmax	Lmin	Lmax	Lmin	Lmax	Lmin	Lmax
L2 (Before 7/16/75)	10.7	225.4	7.4	164.9	7.0	139.3	5.0	138.2
L2 (After 7/16/75)	8.6	282.2	6.3	186.1	6.0	151.3	4.0	130.2
L3 (Before 6/1/78)	4.2	232.3	3.0	175.4	3.1	147.5	1.0	151.7
L3 (After 6/1/78)	4.2	273.5	3.0	179.5	3.1	151.5	1.0	132.1

Table 11.1. Lmin – Lmax table for MSS

The input image data are expected to be floating-point data, derived from samples inherently 7-bit quantization (i.e., 0 to 127 DN). The MSS IAS histogram implementation uses bin width resolutions that are 1/100 of a radiance unit in width based on the input sensor Lmax – Lmin range.

Radiance values lower than Lmin and greater than Lmax should not exist in the image data sets because the original scenes are archived in Qcal space and then converted to spectral radiance using the input sensor Lmin and Lmax values. The database tables should be configured with a validity range corresponding to the smallest Lmin and greatest Lmax expected to be encountered for multiple MSS sensors (i.e., Landsat 2–3), which have P formatted data. Reasonable expansion of this range may make a simpler system design. For example, a Band 4 database validity range of 0 to 300 would be reasonable for both the Landsat 2–3 sensors.

## 11.3 Inputs

- Daytime MSS-P image Bands in spectral radiance space (floating-point)

### 11.3.1 Input Parameters from CPF

- Lmin, Lmax for input sensor

## 11.4 Outputs to Report File and Database

The following are database trending of daytime L1R image data (all Bands) excluding any background fill data (zeros), and/or dropped line fill data (see Section 11.6):

- Band average
- Band standard deviation
- Minimum value
- Maximum value
- Seconds since epoch date
- Date of image acquisition (report file header)
- Number of data values used in band calculations
- Lmin, Lmax
- Input format (A, X, P)

## 11.5 Algorithm Description

This algorithm computes standard first- and second-order statistics using GNU Scientific Library ([GSL](#)) functions for the following parameters:

1. Band average
2. Band standard deviation
3. Band minimum
4. Band maximum

Histogram bin resolution is 1/100 of a radiance unit ( $\text{W}/\text{m}^2 \cdot \text{sr} \cdot \mu\text{m}$ ). All non-image pixels are excluded. All dropped line fill data are excluded.

## 11.6 Issues

1. How to identify dropped lines in the MSS-P data format.
2. Further TBD detector level calculations are expected for MSS-X and MSS-A data. It is unknown at this time if this information will be added to the algorithm module or will invoke reuse of TM / ETM code.



# 12 Histogram Analysis MSS-X Format

## 12.1 Introduction

This algorithm extracts the relevant first- and second-order detector statistics from image data. Depending on the processing level of the input data, these statistics can determine the following:

- Data points for generating relative radiometric calibration models based on time-dependent detector response
- Relative radiometric calibrations specific to the given image

## 12.2 Background

To estimate the relative gains and biases of detectors, characterize the behavior of individual detectors in a band relative to other detectors in a band based on scene content. Individual detector histograms are generated for all scans together. Lines dropped by one detector are excluded from all detectors in that band. As of now, Impulse Noise detection has not been implemented for MSS data. The number of saturated pixels (0 or 127) for each detector is tabulated based on masks generated in the Characterize Detector Saturation function. The detector with the maximum number of saturated pixels in the band is identified; for all other detectors in the band, the same number of brightest or darkest pixels is excluded to provide an equal number of pixels per detector. The means and standard deviations are calculated for each detector from the adjusted histograms and band average mean. The band average standard deviations are calculated, excluding any “dead”, “degraded”, and “inoperable”

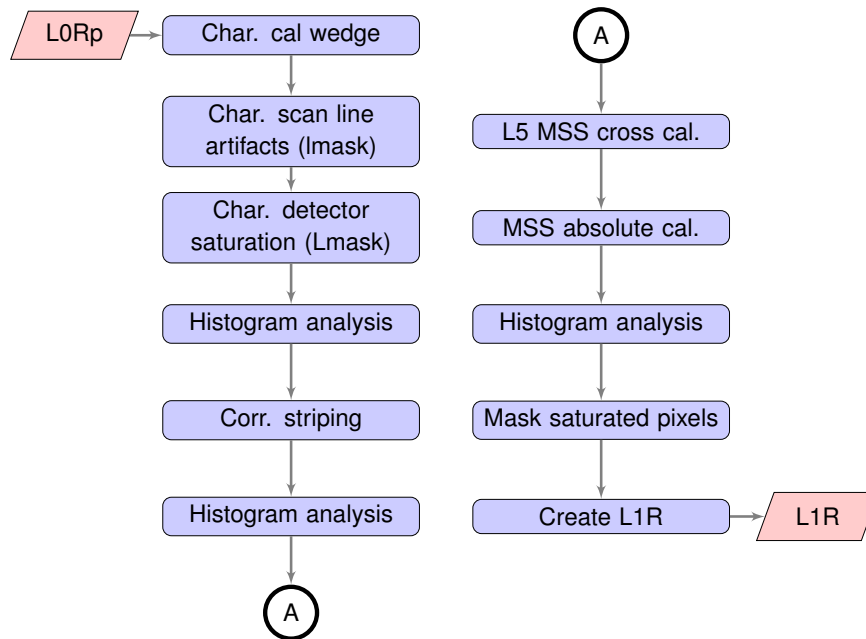


Figure 12.1. MSS Radiometric Processing Flow

detectors. Relative detector-to-detector gains are calculated using two methods; the first method determines ratios of the detector mean to the band average mean and a reference detector mean; and the second method determines ratios of the standard deviations of the detectors to a band average (weighted or unweighted by detector noise levels) standard deviation and a reference detector standard deviation. Bias differences are estimated from a combination of ratios, standard deviations, and mean differences. Filters based on the scene standard deviations relative to the detector noise levels and the overall number of excluded pixels may remove poor scene data from these calculations. This function is performed in its entirety on all MSS-X and MSS-A scenes that IAS processes. For MSS-P scenes, only scene-based statistics are generated.

In general, this algorithm provides a level of functionality similar to the corresponding algorithm in the current Landsat 7 and TM IAS. Like the TM version, this algorithm runs at multiple stages within the main radiometric processing flow.

As currently conceived, this algorithm description is based on the concept of processing data 'levels' in use with the current Landsat 7 IAS. Alternatively, this algorithm can be presented independent of the RPS processing level; in this

manner, modules incorporating specific functionality can be designed, implemented, and called whenever necessary in the process flow. At the time of this writing, it was decided that the algorithm could be more cleanly described relative to processing levels. To determine the exact 'correlation' between specific modules and processing levels, examine the process flow diagrams.

In the Landsat 7 IAS, the image and calibration data are handled as scaled ( $100\times$ ) integer values, and the histograms are computed using unity bin widths. For the TM-IAS, the use of floating-point numbers with no scale factor impacts the required bin widths to achieve sufficient resolution in the histogram statistical calculations. Beginning with R8.0.2, the initial implementation (using unity bin widths) was changed to support 1/100 DN and Radiance bin widths for the histograms, subsequent statistical calculations, and derived relative gain values. Effective with R8.0.3, the histogram calculation dynamic range was extended to 450 counts from 255 to better match the dynamic range of the images throughout the process flow. Starting from R10.3, this dynamic range is also adopted for histogram analysis of MSS data. Histogram results are typically reported as aggregated unity bin width values in the report files and database. In addition, the analog saturation algorithm searches aggregated unity bin width values to determine potential saturation points on both the low and high ends of the dynamic range. Brief update comments are inserted into the following sections to draw the reader's attention where appropriate.

## 12.3 Inputs

- Daytime input Level 0 Reformatted (L0R) (for raw histograms and detector saturation information) (floating-point)
- Daytime Level 0 Reformatted Corrected (L0c) (for relative gain estimation) (floating-point)
- Daytime L1R (for image-specific 'cosmetic' striping removal)(floating-point)
- LMASK

### 12.3.1 Input Parameters from CPF

- Dead / degraded detector information

- Detector noise levels (floating-point)
- Starting pixel for calculation (from Scan Line Offset (SLO) information) (integer)
- Number of pixels for each calculation (window width) (integer)
- Reference detector (integer)
- Saturation bin threshold (integer)
- Adjacent bin threshold (integer)
- Number of adjacent bins to test (integer)

## 12.4 Outputs

Database trending of daytime input (L0R) image data (all bands):

- Detector saturation bins (floating-point)
- Band average, detector level, and summary statistics (mean and standard) for all detectors, including the reference detector (floating-point)

Database trending of daytime L0c / L1R image data (all bands) (can also be used as inputs for scene-specific relative gain correction):

- Detector-specific relative gain ratios to individual reference detector and band-average (floating-point)
- Ratio of standard deviations (floating-point)
- Ratio of means (floating-point)
- Relative bias-calculated with respect to the reference detector and the band-average of all operative detectors (floating-point)
- Number of pixels (integer)
  - Total number used per detector
  - Numbers excluded at both the high-end and low-end of the detector-specific histogram

- Summary histogram statistics for each band (floating-point)
  - Detector means and standard deviations
  - Mean and standard deviation of all operative detectors in the band

Note: Only scene-based trending is applicable for MSS-P data

#### Summary Reporting:

- Daytime L0R, L0c, and L1R histograms (floating-point)
  - Detector-specific
  - Band average (across all operative detectors)
- L0c / L0R scene statistics (floating-point)
- Unweighted / weighted by detector noise (daytime image data)
- Number of high and low brightness pixels excluded (daytime reflective band) (integer)
- Number of pixels used in calculations (integer)
- L0c / L1R computed gain ratios per detector (floating-point)
  - Four sets per window (reference and average, based on mean and standard deviation ratios) (daytime reflective band)
- L0c / L1R computed relative biases per detector (floating-point)
  - Two sets per window (reference and average) (daytime reflective band)
- L0c / L1R differences of gains calculated between the mean ratio and standard deviation ratio (daytime reflective band) (floating-point)
- L0c / L1R differences in relative bias between forward and reverse scans (daytime reflective band image data) (floating-point)
- L0c / L1R ratios of relative gains between forward and reverse scans (daytime reflective band image data) (floating-point )

- L0R saturation bins applicable to L0c image data (daytime reflective band image data) (byte)

Note: Only scene based trending is applicable for MSS-P data

## 12.5 Outputs to Report File and Database

Database trending of daytime L1R image data (all bands) excluding any background fill data (zeros), and/or dropped line fill data (see Section 12.7):

Band Level:

- Band Average
- Band Average per Detector
- Band Standard Deviation
- Band Standard Deviation per Detector
- Minimum Value
- Maximum Value
- Seconds Since Epoch Date
- Number of Data Values used in Band Calculations

Detector Level:

- Scan Averages
- Scan Standard Deviations
- Number of Pixels per Detector Scan used in Histogram Calculations
- Minimum Value per Scan
- Maximum Value per Scan
- Detector Numbers
- Scan Times

## 12.6 Algorithm Description

### 12.6.1 Daytime Input (L0R) Image Data

Within each 'window' of image data that the CPF window parameter defined, perform the following steps:

1. Using the available LMASK information to exclude pixels from dropped lines / scans and detector saturation (0/127 DN) artifacts, generate detector-specific histograms, as well as a band-level histogram over all normally operative detectors. Center the bins at (integer) DN values, and make the bins 1/100 DN in width. After counting the total number of saturated pixels (note: unlike TM, no search for analog saturation is made, excluding them from further histogram calculations), determine the mean and standard deviation. Record these summary statistics in the appropriate report file and trend to the database.

### 12.6.2 L0c / L1R Reflective Band Image Data

Within each 'window' of image data that the CPF window parameter defined, perform the following steps:

1. Following the conversion to radiance (QcalToRadiance) of the input data and using the available LMASK information to exclude dropped lines / scans and detector saturation artifacts, generate detector-specific histograms. From this stage of radiometric processing onward, it is possible that negative DN values were created. Center the bins at (integer) DN values and set the bin widths to 1/100 DN. It is expected that the bin values will range from approximately -5 DN to 10 DN (requiring about 16 aggregated bins for a full characterization). From this high-resolution histogram information, calculate and trend the following summary statistics: minimum, maximum, mean, standard deviation, and total number of pixels. Also, record in the trending database that the statistics came from image data after the conversion to radiance from the input image.
2. Following Correct Striping (if enabled in the processing flow), generate detector-specific histograms. Calculate and trend summary statistics. In addition, record in the database that these statistics came from image data following the striping correction.

- Following the application of cross calibration to Landsat 5 MSS and absolute calibration to Landsat 5 TM, generate detector-specific histograms. From this high-resolution information, calculate and trend the minimum, maximum, mean, standard deviation, and total number of pixels statistics. In addition, record in the database that the statistics came after absolute calibration to applied image data.

### 12.6.3 Daytime L0c/L1R Image Data (all bands)

Within each 'window' of image data that the CPF window parameter defined, perform the following steps:

- Using the available LMASK information to exclude dropped lines / scans and detector saturation artifacts, generate detector-specific histograms for all scans together. Due to the artifact correction, negative DN values can occur. At the higher end, find and convert the largest DN value to the nearest (positive) integer. As with the other histograms generated according to this algorithm, center the bins at (integer) DN values, and set the width to 1/100 DN.
- For each detector, calculate the relative gain defined as the ratio of the mean value to the selected reference source (both the band average and the selected individual reference detector) according to the following:

$$g_i = \frac{\overline{m}_i}{\overline{m}} \quad (12.1)$$

$$g_i = \frac{\overline{m}_i}{m_{ref}} \quad (12.2)$$

where  $m_{ref}$  indicates the mean of the reference detector and  $m$  indicates the band average histogram mean.

- For each detector, calculate the relative gain defined as the ratio of the detector standard deviation to the standard deviation of the reference source (both the band average and the selected individual reference detector) according to the following:

$$g_i = \frac{s_i}{s} \quad (12.3)$$

$$g_i = \frac{s_i}{s_{ref}} \quad (12.4)$$

where  $s_{ref}$  indicates the standard deviation of the reference detector and  $s$  indicates the band average histogram standard deviation.

4. Trend the relative gain results generated in steps 6 and 7. These estimates can also generate lifetime models of relative gain response for each detector.
5. Calculate and trend estimates of relative bias based on the summary statistics calculated in step 3. These estimates are calculated according to the following:

$$b_{rel} = \bar{m} - \bar{s} \frac{m_i}{s_i} \quad (12.5)$$

$$b_{rel} = m_{ref} - s_{ref} \frac{m_i}{s_i} \quad (12.6)$$

6. Weight the band average mean and standard deviation calculated in step 5 with the detector noise level (which is the standard deviation of the L0c calibration shutter region). Do not include dead / degraded detectors in this calculation. Write the results to the appropriate report file.
7. Calculate the ratios and differences of relative gains and biases for both mean-based and standard deviation-based ratios, and write the results to the appropriate report file.



# 13 Cross Calibration to L5 MSS

## 13.1 Introduction

This algorithm calibrates the MSS bands from Landsat 1–5 MSS to ensure consistent radiometric calibration for all sensors. This algorithm is based on the analysis of the [TOA](#) radiance readings from Pseudo-Invariant Calibration Site ([PICS](#)) and near-simultaneously acquired scene pairs that sought to ascertain a gain adjustment solution for each Landsat MSS instrument.

## 13.2 Background

Although each subsequent MSS instrument was calibrated to its predecessor before launch, distinct variances were found within the radiometric archive collection of each satellite. In order to correct these discrepancies, several samples of [TOA](#) radiance over PICS and other near-coincidently acquired scene pairs were collected and analyzed. The scenes used in the analysis spanned across the lifetime of each MSS instrument, and illustrated changes that occurred throughout their operation. This analysis resulted in time-dependent absolute gain adjustment models for the MSS sensors, which were developed to establish radiometric consistency across all five platforms. This analysis had several complications. With operational periods often ending with only one Landsat satellite in the sky, the opportunity to compare each sensor to one another was not readily available. Also, most of the geosynchronous orbits were set at a nine day separation between coincident scene pairs.

Historically, the detector-specific radiance space values were initially calculated by converting into TOA reflectance before the absolute gain adjustments were adjusted. Today, this step can be skipped because the radiance is normalized for the cross calibration absolute gains and biases. The two terms of

Earth-sun distance  $d$  and sun angle  $\theta$  are crucial values in the calculation of TOA reflectance, and should be stored in the database for future use.

The calculation into TOA reflectance is (this equation is for reference only):

$$\rho = \frac{\pi L_{\lambda} d^2}{ESUN_{\lambda} \cos \theta}$$

where  $\rho$  is the TOA reflectance,  $L_{\lambda}$  is the spectral radiance value (units:  $W/m^2 \cdot sr \cdot \mu m$ ),  $d$  is the Earth-sun distance in Astronomical Units (AU),  $ESUN_{\lambda}$  is the mean solar exoatmospheric spectral irradiances ( $W/m^2 \cdot sr \cdot \mu m$ ), and  $\theta$  is the solar zenith angle for the image portion of interest (units: degrees).

Landsat 5 MSS was the destination sensor to map to for several reasons. First, Landsat 5 has the most recent and most complete documentation of all other MSS carrying Landsat satellites. Second, the Landsat 5 MSS detectors have been relatively stable throughout the sensor's entire operational period. Third, Landsat 5 has one of the largest acquisitioned scene counts and longest MSS operational periods, which allows for a better trending model than other MSS sensors. Finally, Landsat 5 has the most recent MSS data. If an effort to scale all of the MSS sensors to Landsat 5 TM is going to occur, scaling the sensors to Landsat 5 MSS is the logical route.

The cross calibration has been completed in the radiance space. The extracted scene radiance values need to be adjusted to account for varying solar illumination conditions among the scenes used in the cross calibration model. The equation of TOA radiance normalization is:

$$L'_{\lambda(Ln)} = L_{\lambda(Ln)} \frac{d^2}{\cos \theta}$$

where  $L'_{\lambda(Ln)}$  is the normalized radiance of Landsat 'n' MSS (units:  $W/m^2 \cdot sr \cdot \mu m$ ),  $L_{\lambda(Ln)}$  is the original radiance value of Landsat 'n' MSS (units:  $W/m^2 \cdot sr \cdot \mu m$ ),  $d$  is the Earth-sun distance in AU, and  $\theta$  is the solar zenith angle for the image portion of interest (units: degrees).

In order to accomplish a radiometric consistency through a "grapevine" method, Landsat 1 MSS was cross calibrated to Landsat 2 MSS, Landsat 2 MSS to Landsat 3 MSS, Landsat 3 MSS to Landsat 4 MSS, and Landsat 4 MSS to Landsat 5 MSS. In this method, several sets of two (nearly) coincident scenes were matched in PICS, and several regions of interest were sampled to estimate relationships between the gains of two sensors. The cross calibration

to Landsat 5 for each sensor was calculated by combining results of individual cross-calibrations between sensor pairs. This cross calibration process revealed an existence of statistically significant cross calibration biases for some bands in some sensors. In addition, some bands showed statistically significant gain changes throughout the lifetime of the associated sensors.

To account for change in gain over the mission lifetime, a Time-Dependent Factor (TDF) term was added to the final cross calibration equation. This TDF is defined as:

$$\text{TDF} = \frac{C}{A(T - T_{\text{launch}}) + B}$$

where  $C$  is the normalized radiance of the reference PICS at the cross calibration time point (units:  $\text{W}/\text{m}^2 \cdot \text{sr} \cdot \mu\text{m}$ ),  $T$  is the scene acquisition date (units: decimal years),  $T_{\text{launch}}$  is the satellite launch date (units: decimal years),  $A$  is the regression slope of the gain versus time model (units:  $\text{W}/(\text{m}^2 \text{ sr } \mu\text{m decimal years})$ ), and  $B$  is the bias derived from the regression offset of the gain versus time model (units:  $\text{W}/\text{m}^2 \cdot \text{sr} \cdot \mu\text{m}$ ).

For example, assume that the gain change with time for Landsat 2 MSS is characterized through apparent change in radiance of the reference calibration site as:

$$L_2 = 0.567092T - 975.194$$

If the cross calibration point for Landsat 2 MSS and Landsat 3 MSS is 1980.13 years and the launch date of Landsat 2 is 1975.06 years, then

$$A = 0.567092 \text{W}/(\text{m}^2 \text{ sr } \mu\text{m decimal years})$$

$$B = 0.567092 \times 1975.06 - 975.194 = 144.847 \text{W}/\text{m}^2 \cdot \text{sr} \cdot \mu\text{m}$$

$$C = 0.567092 \times (1980.13) - 975.194 = 147.722 \text{W}/\text{m}^2 \cdot \text{sr} \cdot \mu\text{m}$$

For bands in which the gain does not change with time,  $A$  needs to be set to 1,  $B$  to 0, and  $C$  to 1.

The radiance acquired by any MSS sensor as if it were acquired by Landsat 5 MSS can be estimated using the final cross calibration equation:

$$L_{\lambda(L5)} = G_{n,5} L_{\lambda(Ln)} \text{TDF} + b_{n,5}$$

where  $L_{\lambda(L5)}$  is the Landsat 5 MSS mapped radiance value (units:  $\text{W}/\text{m}^2 \cdot \text{sr} \cdot \mu\text{m}$ ),  $G_{n,5}$  is the cross calibration gain between the given band, the MSS sensor, and the Landsat 5 MSS (unitless),  $L_{\lambda(Ln)}$  is the original radiance value of

Landsat 'n' MSS (units:  $W/m^2 \cdot sr \cdot \mu m$ ), and  $b_{n,5}$  is the cross calibration band offset from Landsat 5 MSS (units:  $W/m^2 \cdot sr \cdot \mu m$ ).

For example, if TDF =1 and the cross-calibrations between sensor pairs for a given spectral band are estimated as:

$$\begin{aligned} L_5 &= G_4 L_4 \\ L_4 &= G_3 L_3 \\ L_3 &= G_2 L_2 + b_2 \\ L_2 &= G_1 L_1 + b_1 \end{aligned}$$

Then,

$$\begin{aligned} L_{\lambda(L5)} &= G_3 G_4 L_3 \\ &= G_3 G_4 G_2 L_2 + G_3 G_4 b_2 \\ &= G_3 G_4 G_2 G_1 L_1 + G_3 G_4 G_2 b_1 + G_3 G_4 b_2 \end{aligned}$$

Thus,

$$\begin{aligned} G_{4,5} &= G_4, & b_{4,5} &= 0 \\ G_{3,5} &= G_3 G_4, & b_{3,5} &= 0 \\ G_{2,5} &= G_2 G_3 G_4, & b_{2,5} &= G_3 G_4 b_2 \\ G_{1,5} &= G_1 G_2 G_3 G_4, & b_{1,5} &= G_3 G_4 G_2 b_1 + G_3 G_4 b_2 \end{aligned}$$

The TOA reflectance for scenes acquired by any MSS sensor can be calculated as:

$$\rho = \frac{\pi L_{\lambda(L5)} d^2}{ESUN_{\lambda(L5)} \cos \theta}$$

where  $\rho$  is the TOA reflectance,  $L_{\lambda(L5)}$  is the radiance mapped to Landsat 5 MSS (units:  $W/m^2 \cdot sr \cdot \mu m$ ),  $d$  is the Earth-sun distance in [AU](#),  $ESUN_{\lambda(L5)}$  is the mean solar exoatmospheric spectral irradiance for Landsat 5 MSS ( $W/m^2 \cdot sr \cdot \mu m$ ), and  $\theta$  is the solar zenith angle for the image portion of interest (units: degrees).

### 13.3 Inputs

- MSS image radiance space data (floating-point)

## 13.4 Parameters Obtained From the CPF

- Estimated cross calibration gains
- Estimated cross calibration biases
- Time dependent factors  $A$ ,  $B$ ,  $C$ , and  $T_{\text{launch}}$

## 13.5 Outputs

- Landsat 5 MSS mapped radiance space image data (floating-point)

## 13.6 Database

- Final cross calibration gain value
- Applied bias values
- Acquisition time stamp
- Solar zenith angle
- Calculated sun distance

## 13.7 Algorithm

Image data must be in spectral radiance space before running this algorithm on the floating-point image data.

Taking into account that the cross calibration gains are derived from normalized radiance and that the TDF is calculated as:

$$\text{TDF} = \frac{C}{A(T - T_{\text{launch}}) + B}$$

where  $C$  is the normalized radiance of the reference [PICS](#) at the cross calibration time point (units:  $\text{W}/\text{m}^2 \cdot \text{sr} \cdot \mu\text{m}$ ),  $T$  is the scene acquisition date (units: decimal years),  $T_{\text{launch}}$  is the satellite launch date (units: decimal years),  $A$  is

the regression slope of the gain versus time model (units:  $W/m^2 \cdot sr \cdot \mu m$  decimal years)), and  $B$  is the bias derived from the regression offset of the gain versus time model (units:  $W/m^2 \cdot sr \cdot \mu m$ ).

The final equation is:

$$L_{\lambda(L5)} = G_{n,5} L_{\lambda(Ln)} TDF + b_{n,5}$$

where  $L_{\lambda(L5)}$  is the Landsat 5 MSS mapped radiance value (units:  $W/m^2 \cdot sr \cdot \mu m$ ),  $G_{n,5}$  is the cross calibration gain between the given band, the MSS sensor, and the Landsat 5 MSS (unitless),  $L_{\lambda(Ln)}$  is the original radiance value of Landsat 'n' MSS (units:  $W/m^2 \cdot sr \cdot \mu m$ ),  $b_{n,5}$  is the cross calibration band offset from Landsat 5 MSS (units:  $W/m^2 \cdot sr \cdot \mu m$ ), and TDF is the time dependent factor.

# 14 Absolute Gain and Offset Adjustment

## 14.1 Introduction

This algorithm calibrates the cross calibrated MSS bands to the Landsat 5 TM sensor. The Landsat 5 TM sensor is absolute-calibrated. A cross calibration of the MSS sensors to TM offers an absolute radiometric calibration for the MSS sensors. Historically, the MSS sensor incorporates an Internal Calibrator (IC) system to determine the gain and bias of all bands (1–4). Not knowing the degradation effects of the IC response, post-calibration adjustments for the MSS sensors are needed.

Cross calibration incorporates adjustments for spectral band differences and spatial differences between the sensors. Each MSS absolute calibration gain carries an uncertainty of 1.2 percent to 3.0 percent with respect to TM. In order to distinguish the absolute calibration changes from the MSS cross calibration changes in each of the processed scenes, an additional CPF value field has been created. This field holds absolute calibration independent of the existing radiometric calibration system, and allows production the opportunity to turn off this step if needed.

## 14.2 Background

For both the MSS and the TM sensors, an onboard IC system observed the radiometric performance of the sensor. The IC degraded in space with no independent means of monitoring this calibration system degradation. Therefore, an alternative calibration method is needed for the sensors. The TM sensor on board Landsat 5 provides an enhanced spatial, spectral, radiometric, and geo-

metric performance compared to the MSS sensor. With greater sophistication, the TM sensor relied on multiple calibration techniques throughout its lifetime. These techniques include cross calibration with Landsat 7 ETM+ (Teillet et al 2001), vicarious measurements, and detector responses to the IC. The Landsat 5 TM radiometric calibration uncertainty of the at-sensor spectral radiance is estimated to average five percent.

Radiometric cross calibration of each sensor was completed using near-simultaneous imaging of a known PICS. The overlap of Landsat 5 MSS and TM sensor is eight years, creating coincidental scene pairs from 1984 to 1992. During this time period, 32,318 scenes were archived, which provides a great opportunity for cross calibration.

For the cross calibration of Landsat 5 MSS to Landsat 5 TM, the PICS site of the Sonora Desert in Mexico was used. This area was a preferable location because of the readily available MSS, TM, and Hyperion scene coverage and the flat homogeneous reflectance of this area. Within this area, three spectrally flat Regions of Interest (ROIs) were chosen to maximize the comparison between the MSS and TM. Using the high spectral resolution of the Hyperion sensor, the spectral signature of each ROI was obtained. Through the known spectral signatures and spectral responses of both the MSS and TM sensors, spectral differences between the two can be calculated.

## 14.3 Methodology

The absolute calibration of MSS to Landsat 5 TM includes an adjustment to the MSS absolute gains, and an addition of a Spectral Band Adjustment Factor (SBAF). This SBAF is specific to each reflective surface, and is not supplied to the end user through the means of the IAS. Each end-user applies their own SBAF value in accordance to what they are studying or interested in when comparing the MSS and TM sensors. The SBAF correction factor must be applied to MSS data for it to be absolutely calibrated. This is true for all reflective surfaces, including desert sites.

To verify the absolute calibration between Landsat 5 TM and the cross calibrated MSS instruments, several coincidental collects over a PICS were analyzed. This was performed for Landsat 4 MSS to TM and Landsat 5 MSS to TM sensors. The cross-comparisons of Landsat 5 TM to Landsat 4 TM and Landsat 5 MSS to Landsat 4 MSS were also taken into account in order to ensure consistency between the absolute calibration values.

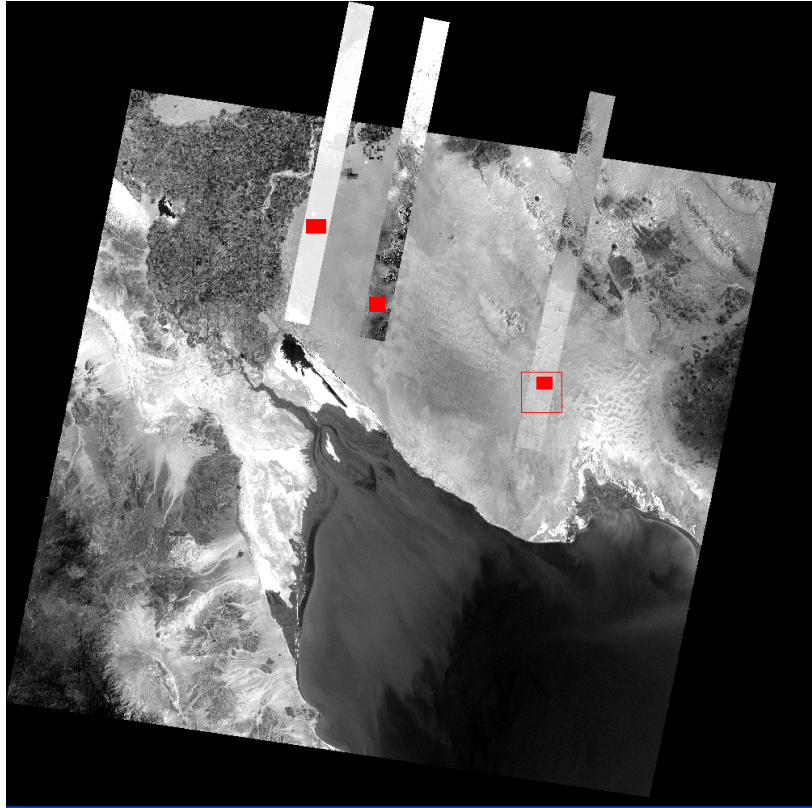


Figure 14.1. Mosaic Image of a TM Scene and Three Hyperion Scenes used in Cross Calibration<sup>a</sup>

<sup>a</sup>The red boxes are the ROIs chosen for Cross Calibration

The absolute calibration equations of TOA radiance are:

$$\begin{aligned} L_{MSS4\lambda} &= L_{TM5\lambda} G_{TM5 \rightarrow MSS5} SBAF_{TM5 \rightarrow MSS5} G_{MSS5 \rightarrow MSS4} \\ &= L_{TM5\lambda} G_{TM5 \rightarrow TM4} G_{TM4 \rightarrow MSS4} SBAF_{TM4 \rightarrow MSS4} \end{aligned}$$

$$\begin{aligned} \therefore G_{TM5 \rightarrow TM4} G_{TM4 \rightarrow MSS4} SBAF_{TM4 \rightarrow MSS4} \\ = G_{TM5 \rightarrow MSS5} G_{MSS5 \rightarrow MSS4} SBAF_{TM5 \rightarrow MSS5} \quad (14.1) \end{aligned}$$

where  $L_{MSS'n'\lambda}$  is the at-sensor radiance of Landsat 'n' MSS Band  $\lambda$  (units:  $W/m^2 \cdot sr \cdot \mu m$ ),  $L_{TM'n'\lambda}$  is the at-sensor radiance of Landsat 'n' TM (units:  $W/m^2 \cdot sr \cdot \mu m$ ),  $G_{X \rightarrow Y}$  is the gain for sensor  $X$  to sensor  $Y$  (unitless), and  $SBAF_{X \rightarrow Y}$

is the **SBAF** converting sensor  $X$  to sensor  $Y$  for a target with moderately flat spectral response (unitless).

The end result of this methodology is the addition of a final gain applied to existing Landsat 5 MSS radiance values. The absolute gain for each Landsat 5 MSS Band is based on the absolute calibrated Landsat 5 TM corresponding band. The final equation for applying the absolute gain is as follows:

$$L_{TM^*\lambda} = G_{\lambda}L_{MSS\lambda}$$

where  $L_{MSS\lambda}$  is the at-sensor radiance of Landsat 5 MSS Band  $\lambda$  (units:  $W/m^2 \cdot sr \cdot \mu m$ ),  $L_{TM^*\lambda}$  is the at-sensor radiance of Landsat 5 TM Band  $\lambda$  (units:  $W/m^2 \cdot sr \cdot \mu m$ ), and  $G_n$  is the gain for converting MSS Band  $\lambda$  to the corresponding TM Band  $\lambda$  from the CPF (unitless).

For example, if current MSS Band 1 radiometric data was converted to absolute radiance, based on Landsat 5 TM Band 2 (the TM's corresponding Band), the equation would be applied as follows:

$$\begin{aligned} L_{TM^*2} &= G_1L_{MSS1} \\ &= 0.83L_{MSS1} \end{aligned}$$

A 0.83 gain is applied to the MSS Band 1 radiance data. The new value is in absolute radiance based on Landsat 5 TM Band 2.

## 14.4 Inputs

- Cross-calibrated MSS image radiance space data (floating-point)

## 14.5 Parameters Obtained From the CPF

- Estimated absolute calibration gains ( $G_{n,n+1}$ )

## 14.6 Outputs

- Landsat 5 TM mapped radiance space image data (floating-point)

## 14.7 Algorithm

The final equation is:

$$L_{TM\lambda}(L_{nTM}) = G_{n,n+1}L_{MSS\lambda}(L_{nMSS})$$

where  $L_{MSS\lambda}$  is the at-sensor radiance of Landsat 'n' MSS Band  $\lambda$  (units:  $W/m^2 \cdot sr \cdot \mu m$ ),  $L_{TM'n'\lambda}$  is the at-sensor radiance of Landsat 'n' TM (units:  $W/m^2 \cdot sr \cdot \mu m$ ), and  $G_{n,n+1}$  is the gain for converting MSS Band 'n' to the corresponding TM Band 'n + 1' from CPF(unitless).



# 15 Cosmetic De-Stripping

## 15.1 Introduction

The cosmetic striping algorithm removes small residual offsets between detectors due either to small inherent detector sensitivity differences or imbalances introduced in prior processing steps. This algorithm is executed on MSS-X and MSS-A data after converting to floating-point radiance data from the input Qcal data. The applied correction factors are derived from histogram analysis executed immediately prior to this algorithm in the process flow. The applied correction factors are unique to the scene being processed, rather than being based on a lifetime sensor model or other extended characterizations. Unlike TM data, this routine is executed by default; however, the correction for individual bands can be disabled if a final striping correction is not desired.

## 15.2 Background

In this algorithm, the data are linearly adjusted to match the means and standard deviations of each detector to a reference detector or an average of the detectors.

## 15.3 Input Parameters from CPF

- Scene Data – Normal Earth scenes (all Bands) (floating-point)
- Correction relative gains (floating-point, unitless) and bias (floating-point) from histogram analysis performed on data after converting to floating-point radiance data from the input Qcal data. For relative gains, use

the band average or reference detector for normalization. These values originate as outputs from the HistoAnalysisChar routine.

## 15.4 CPF Parameters

```
Group = Striping
  Correction_Reference_B4
  Correction_Reference_B5
  ...
  Correction_Reference_B7
End_Group = Striping
```

Three options exist for setting the correction reference for each band as follows:

- 0:** Band Average Calculations
- 1:** Use Reference Detector
- 2:** No Correction is Applied

```
Group = Histogram
  Reference_Detector_B4
  Reference_Detector_B5
  ...
  Reference_Detector_B7
End_Group = Histogram
```

The reference detector for each band may be set for any valid detector from 1 to 6.

## 15.5 Outputs

- De-striped image data (floating-point)

## 15.6 Algorithm Description

This algorithm applies the relative gains and relative bias that the HistoAnalysis-Char analysis procedure calculated. The relative gains are calculated by ratioing the standard deviations. The application procedure is similar to the standard de-stripping Land Analysis System (LAS) algorithm, “DESTRIPE,” although the correction gains and bias are calculated differently. (Note: “DESTRIPE” calculates and applies correction factors). The application of these gains and biases, per detector per band, is expressed as follows:

$$Q_{\text{cor}} = \frac{Q_{\text{uncorr}}}{\text{GAIN}_{\text{rel}}} + \text{BIAS}_{\text{rel}}$$

Where  $Q_{\text{cor}}$  is the corrected quantized radiance,  $\text{GAIN}_{\text{rel}}$  is the relative gain factor per detector, from the histogram analysis program based on the ratios of the individual detector standard deviations to the standard deviation of either the band average or reference detector,  $Q_{\text{uncorr}}$  is the uncorrected quantized radiance, and  $\text{BIAS}_{\text{rel}}$  is the relative bias per detector, determined by the histogram analysis program relative to either the average or reference detector.



# Appendices



# Acronyms

<b>ADD</b>	Algorithm Description Document
<b>AFOV</b>	Angular Field of View
<b>AU</b>	Astronomical Units
<b>BIL</b>	Band Interleaved by Line
<b>BIP</b>	Band Interleaved by Pixel
<b>BIP2</b>	Band Interleaved by Pixel Pair
<b>BSQ</b>	Band Sequential
<b>CDR</b>	Calibration Data Record
<b>CPF</b>	Calibration Parameter File
<b>DN</b>	Digital Number
<b>EROS</b>	Earth Resource Observation and Science
<b>ETM+</b>	Enhanced Thematic Mapper Plus
<b>GSFC</b>	Goddard Space Flight Center
<b>GSL</b>	GNU Scientific Library
<b>IAS</b>	Image Assessment System
<b>IC</b>	Internal Calibrator
<b>IFOV</b>	Instantaneous Field of View

<b>L1</b>	Level 1
<b>LAS</b>	Land Analysis System
<b>LPGS</b>	Level 1 Product Generation System
<b>MACS</b>	MSS-X Archive Conversion System
<b>MSS</b>	Multispectral Scanner
<b>PICS</b>	Pseudo-Invariant Calibration Site
<b>ROI</b>	Region of Interest
<b>RPS</b>	Radiometric Processing Subsystem
<b>SBAF</b>	Spectral Band Adjustment Factor
<b>SLA</b>	Scan Line Artifact
<b>SLO</b>	Scan Line Offset
<b>TDF</b>	Time-Dependent Factor
<b>TM</b>	Thematic Mapper
<b>TOA</b>	Top of Atmosphere
<b>USGS</b>	United States Geological Survey
<b>WBVT</b>	Wide-Band Video Tape

## References

- [Bhatt, 2009] Bhatt, R. (2009). Consistent radiometric calibration of landsat-1 through -5 mss sensors using pseudo-invariant calibration sites. Masters thesis.
- [Helder, 1993] Helder, D. (1993). MSS radiometric calibration handbook. Technical report, South Dakota State University.
- [Helder et al., 2004] Helder, D., Ruggles, T. A., Dewald, J. D., and Madhavan, S. (2004). Landsat-5 thematic mapper reflective-band radiometric stability. *IEEE Transaction on Geoscience and Remote Sensing*, 42(12):17.
- [Jasinski, 2010] Jasinski, B. (2010). Consistent absolute calibration of landsat 1-5 multispectral scanner. Technical report.
- [Morstad and Helder, 2008] Morstad, D. L. and Helder, D. L. (2008). Use of pseudo-invariant sites for long-term sensor calibration.
- [Space and Communications Group, 1972] Space and Communications Group, H. A. C. (1972). Multispectral scanner system for erts four band scanner system. System description and performance, NASA.
- [Uprety, 2009] Uprety, S. (2009). *Radiometric Stability Analysis of Landsat-1 through -5 MSS Sensors*. PhD thesis.
- [USGS, 2003] USGS (2003). Landsat 7 image assessment system (IAS) radiometric algorithm theoretical basis document (ATBD). Technical Report LS-IAS-02. Version 1.0.